Supporting Information

7-Deaza-2'-deoxyguanosine: Selective Nucleobase Halogenation, Positional Impact of Space-Occupying Substituents and Stability of DNA with Parallel and Antiparallel Strand Orientation

Sachin A. Ingale[†] and Frank Seela*[†‡]

[†]*Laboratory of Bioorganic Chemistry and Chemical Biology, Center for Nanotechnology, Heisenbergstraße 11, 48149 Münster, Germany and* [‡]*Laboratorium für Organische und Bioorganische Chemie, Institut für Chemie neuer Materialien, Universität Osnabrück, Barbarastraße 7, 49069 Osnabrück, Germany*

Table of Contents

Table S1. ^{13}C NMR Chemical Shifts of 7-Deazapurine Derivatives[a]

	C2[b] C2[c]	C6[b] C4[c]	C5[b] C4a[c]	C7[b] C5[c]	C8[b] C6[c]	C4[b] C7a[c]	CH/CH$_3$/OCH$_3$/C=O	Phenyl-C7 Phenyl-C5	C1'	C2'	C3'	C4'	C5'
1a[19]	151.9	157.2	103.7	112.9	71.5	151.3	-	-	86.9	37.5	71.3	87.4	62.3
6	152.0	157.2	103.7	73.1	112.8	151.3	-	-	92.0	70.8[d]	70.4[d]	85.1	62.3
2	151.8	158.1	100.8	102.2	133.0	151.2	-	132.0, 128.6, 128.2, 127.3	83.9	37.0	70.9	87.0	61.9
10	145.8	156.2	104.6	102.9	135.7	148.5	34.4/18.6/-/179.7	131.6, 129.0, 128.2, 127.9	83.2	36.4	70.4	86.6	61.4
11	145.9	156.5	105.0	103.0	135.9	148.6	34.6/18.8/54.9/179.8	131.8[d], 129.8[d], 129.6[d], 127.5[d]	83.9	37.5	71.0	85.8	64.8
8[6a]	147.5	156.1	104.0	55.7	124.3	147.1	34.7/18.8/-/180.0	-	82.6	-[e]	70.8	87.3	61.7
9	146.3	154.8	107.6	89.6	74.2	148.9	34.7/18.9/-/180.1	-	87.2	37.3	70.9	87.2	62.0
3[22]	152.6	158.8	97.2	120.1	115.0	151.9	-	134.3, 127.8, 127.6, 125.6	82.1	-[e]	71.0	87.0	62.0
13	146.9	156.8	101.0	120.6	117.4	148.7	34.7/18.9/-/180.0	133.6, 128.0, 127.8, 126.1	82.4	-[e]	70.8	87.3	61.8
14	147.0	156.8	101.2	120.8	117.1	148.8	34.7/18.9/54.9/180.0	133.3[d], 127.9[d], 127.7[d], 126.1[d]	82.5	-[e]	70.9	85.6	64.1
4	152.9	159.0	96.8	109.0	114.2	151.5	-	130.0, 128.5 120.3, 120.1	82.3	-[e]	71.1	87.1	62.0
19	147.3	157.1	101.0	109.8	116.4	148.4	34.8/18.9/54.9/180.1	130.0[d], 128.7[d] 120.6[d], 120.1[d]	82.6	-[e]	70.5	85.4	64.0

[a] Measured in DMSO-d_6 at 298 K. [b] Purine numbering. [c] Systematic numbering. [d] Tentative. [e] Superimposed by DMSO.

Table S2. ^{1}H-^{13}C Coupling Constants (Hz) of 7-Deaza-2'-deoxyguanosine Derivatives[a,b]

	***J* [Hz]**									
	6	**9**	**2**	**10**	**11**	**3**	**13**	**14**	**4**	**19**
^{3}J(C7a, H-C5) or ^{3}J(C7a, H-C1')	5.4	4.5	5.9	6.6	6.6	-	-	-	-	-
^{3}J(C7a, H-C6) or ^{3}J(C7a, H-C1')	-	-	-	-	-	8.9	6.0	7.9	5.8	8.3
^{2}J(C4a, H-C5) ^{2}J(C4a, H-N1)	3.5	3.5	3.4	3.4	3.5	-	-	-	-	-
^{3}J(C4a, H-C6)	-	-	-	-	-	6.5	5.9	7.3	-	6.1
^{2}J(C5, H-C6)	-	-	-	-	-	4.7	4.5	5.0	5.3	5.3
^{1}J(C5, H-C5)	179.8	-	175.0	176.8	176.7	-	-	-	-	-
^{1}J(C6, H-C6)		-	-	-	-	187.7	189.2	190.5	191.0	192.8
^{1}J(C1', H-C1')	157.4	160.1	159.8	160.1	164.1	163.8	164.2	167.1	166.3	164.2
^{1}J(C3', H-C3')	148.6	148.7	151.5	150.1	149.2	150.8	150.3	148.3	146.3	152.6
^{1}J(C4', H-C4')	148.9	150.7	148.7	147.2	148.3	147.6	145.6	147.3	146.2	148.5
^{1}J(C5', H-C5')	137.3	139.9	140.3	140.6	142.9	139.2	139.2	141.1	140.0	143.1

[a] Measured in DMSO-d_6 at 298 K. [b] Systematic numbering.

Table S3. Selected Chemical Shifts of 7-Deaza-2´-deoxyguanosine Derivatives.[a,b]

Signal	7-Deaza-dG (1)	7-Iodo-7-deaza-dG (1b)	7-Phenyl-7-deaza-dG (3)	8-Iodo-7-deaza-dG (1a)	8-Phenyl-7-deaza-dG (2)
C1´	82.2	81.9	82.1	86.9	83.9
C2´	39.2	-[c]	-[c]	37.5	37.0
C3´	70.8	70.6	71.0	71.3	70.9
C4´	86.9	86.8	87.0	87.4	87.0
C5´	61.9	61.6	62.0	62.3	61.9
C7	102.1	54.7	120.1	112.9	102.2
C8	116.7	121.4	115.0	71.5	133.0
H1´	6.30	6.24	6.38	6.19	6.08
H2´´	2.07	2.05	2.10	2.01	1.90
H2´	2.33	2.29	2.42	3.14	3.01
H3´	4.29	4.24	4.31	4.38	4.21
H4´	3.75	3.73	3.77	3.77	3.71
H5´	3.47	3.45	3.51	3.60	3.55
OH3´	5.18	5.18	5.21	5.22	5.05
OH5´	4.90	4.88	4.91	5.04	5.12
H7	6.25	-	-	6.56	6.27
H8	6.90	7.09	7.27	-	-

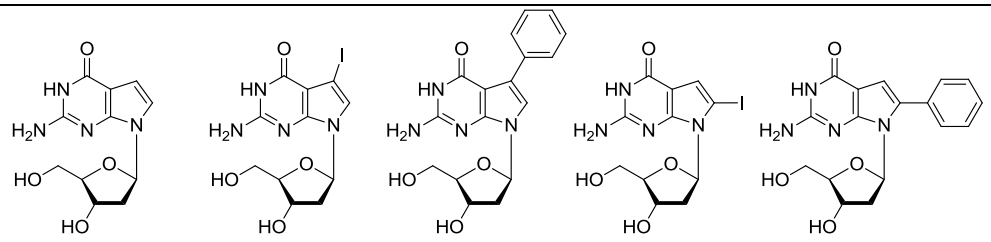

1 **1b** **3** **1a** **2**

[a] Measured in DMSO-d_6 at 298 K. [b] Purine numbering. [c] Superimposed by DMSO-d_6.

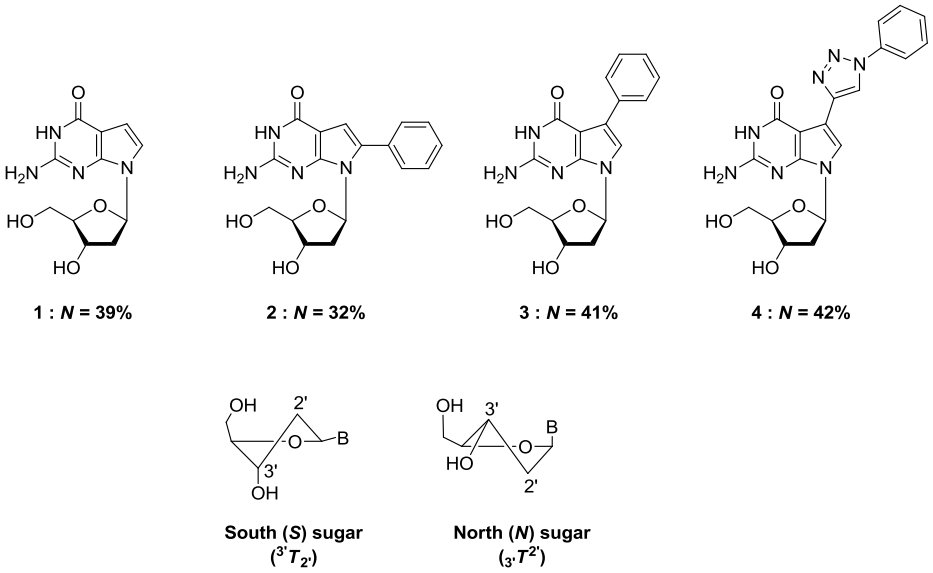

Figure S1. Conformer population of nucleosides **1-4** determined in DMSO-d_6. The conformational analysis of the sugar moiety in solution was performed using the program PSEUROT (version 6.3). The input used the following coupling constants: ^3J(H1´, H2´), ^3J(H1´, H2´´),^3J(H2´, H3´), ^3J(H2´´, H3´), ^3J(H3´, H4´). B = base.

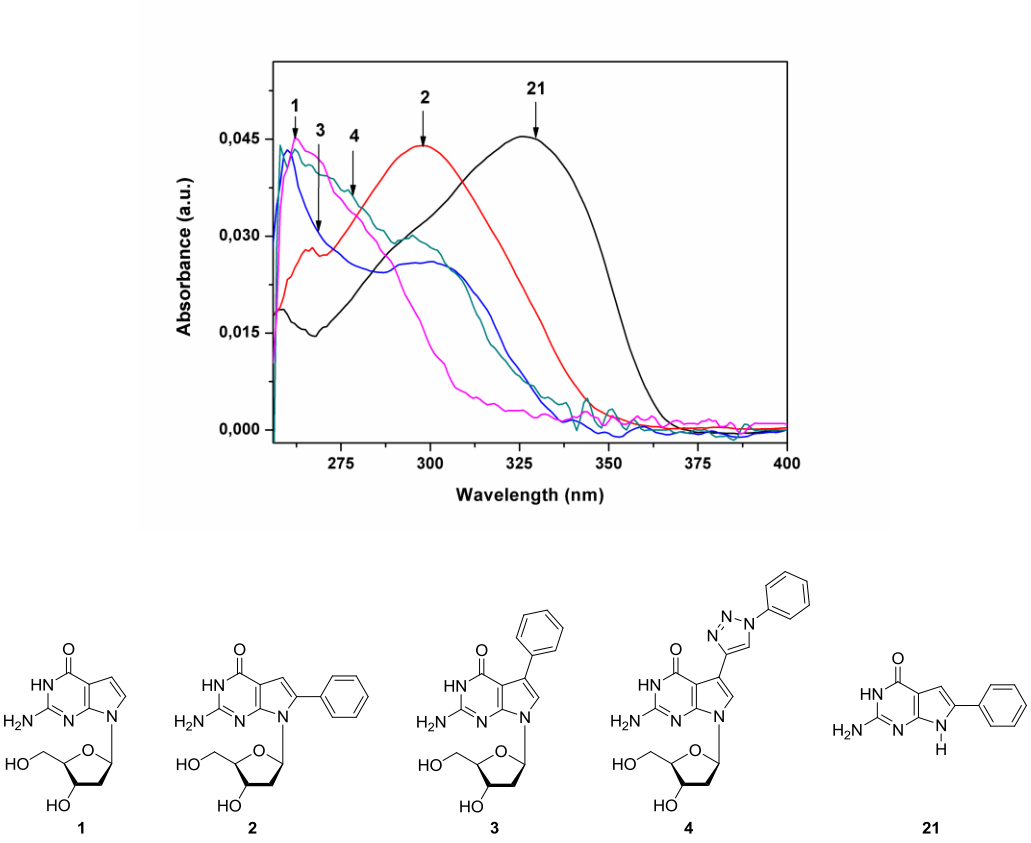

Figure S2. UV/vis spectrum of nucleosides **1-4** and nucleobase **21** (2 µM) in DMSO.

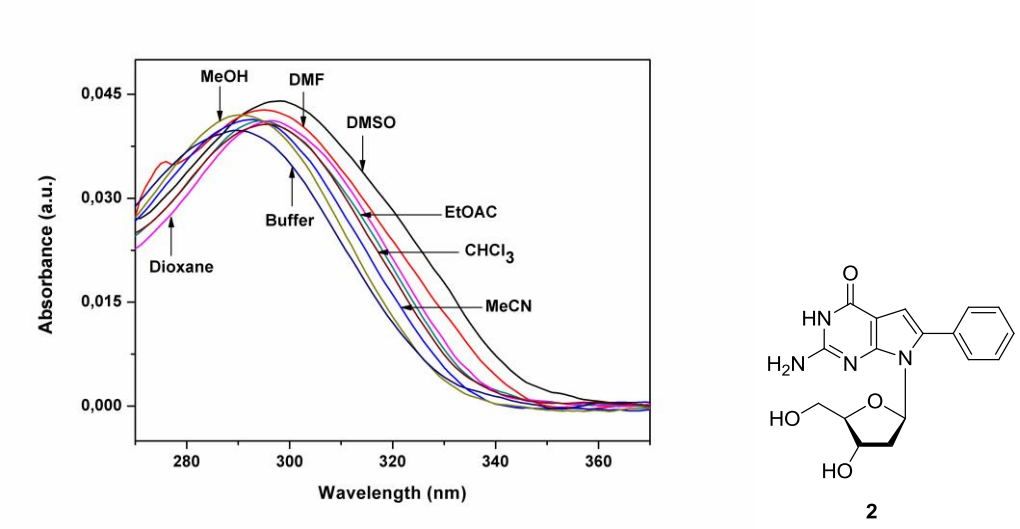

Figure S3. UV-Visible spectrum of nucleoside **2** (2 µM) in various solvents.

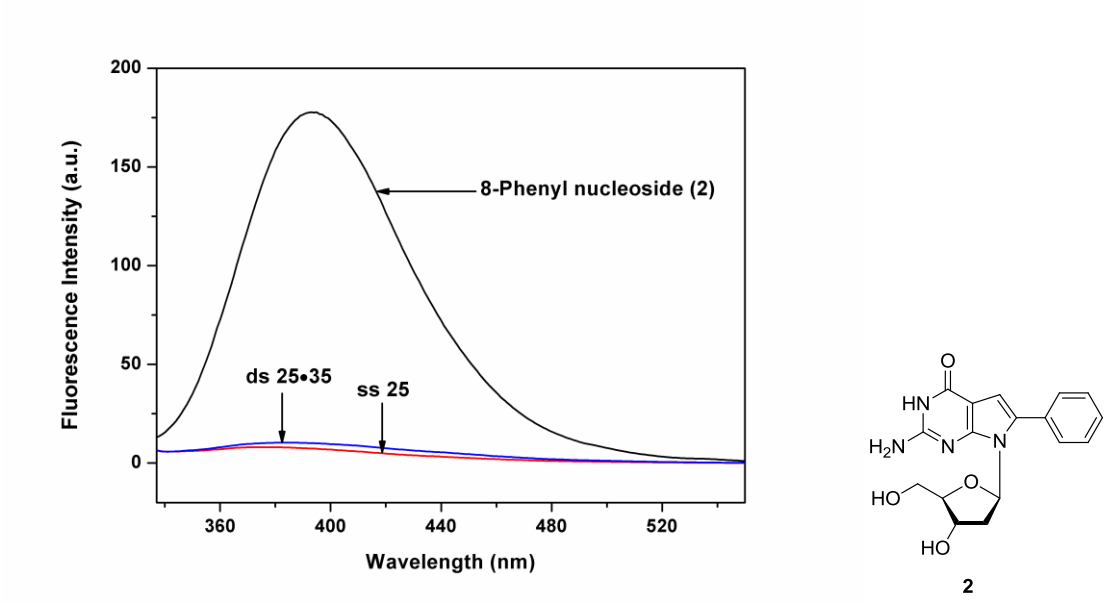

5'-d(TA**2** GTC AAT ACT) (**25**)

5'-d(TA**2** GTC AAT ACT) (**25**)
3'-d(ATC CAG TTA TGA) (**35**)

Figure S4. Fluorescence emission spectra of 2 µM of 8-phenyl nucleoside **2**, 2 µM single stranded (ss) oligonucleotide (**25**) and corresponding double stranded (ds) oligonucleotide (**25•35**, 2 µM of each strand) measured in 1 M NaCl, 100 mM $MgCl_2$, and 60 mM Na-cacodylate buffer (pH 7.0).

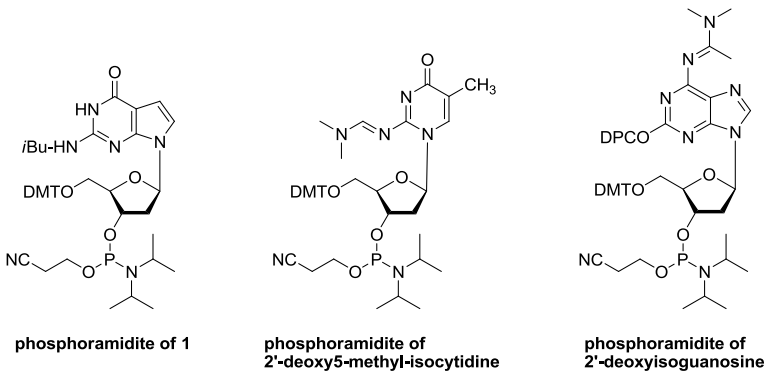

Figure S5. Structures of phosphoramidites.

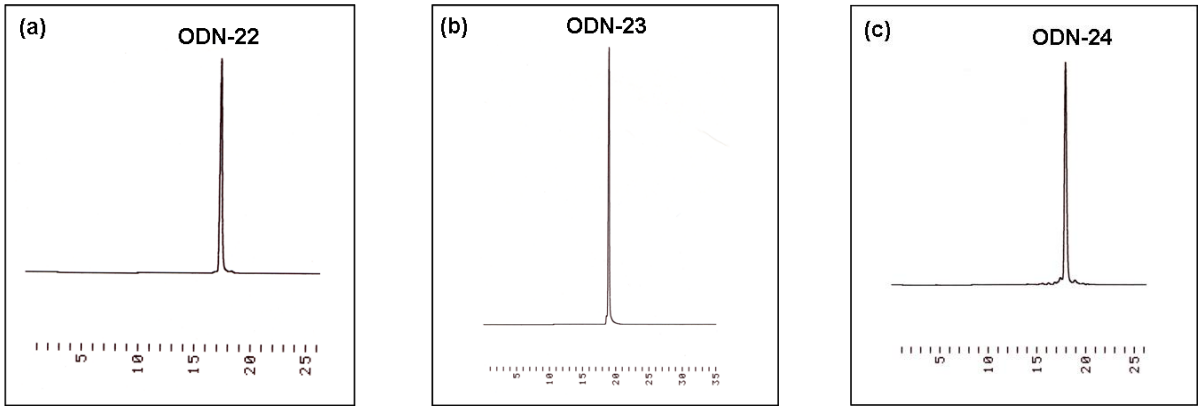

Figure S6. Reversed-phase HPLC profiles of purified single-stranded oligonucleotides containing 7-deaza-2'-deoxyguanosine determined at 260 nm, (a) ODN-**22**; (b) ODN-**23**; (c) ODN-**24**. For elution the following solvent system was used: (A) MeCN and (B) 0.1 M $(Et_3NH)OAc$ (pH 7.0): MeCN (95:5). Gradient II: 0-20 min 0-20% A in B, 20-25 min 20% A in B, flow rate 0.8 mL/min. X-axis corresponds to retention time [min] and y-axis corresponds to UV absorbance at 260 nm.

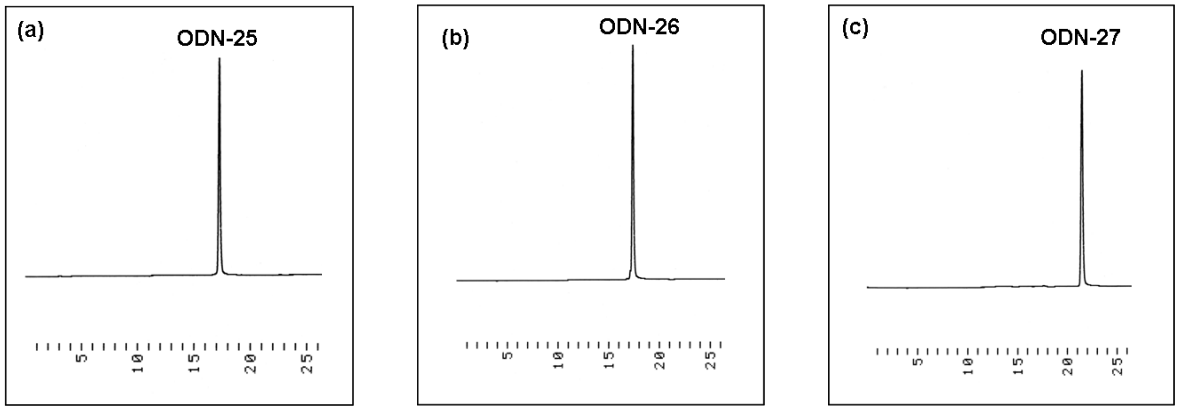

Figure S7. Reversed-phase HPLC profiles of purified single-stranded oligonucleotides containing 8-phenyl-7-deaza-2'-deoxyguanosine determined at 260 nm, (a) ODN-**25**; (b) ODN-**26**; (c) ODN-**27**. For elution the following solvent system was used: (A) MeCN and (B) 0.1 M (Et_3NH)OAc (pH 7.0): MeCN (95:5). Gradient II: 0-20 min 0-20% A in B, 20-25 min 20% A in B, flow rate 0.8 mL/min. X-axis corresponds to retention time [min] and y-axis corresponds to UV absorbance at 260 nm.

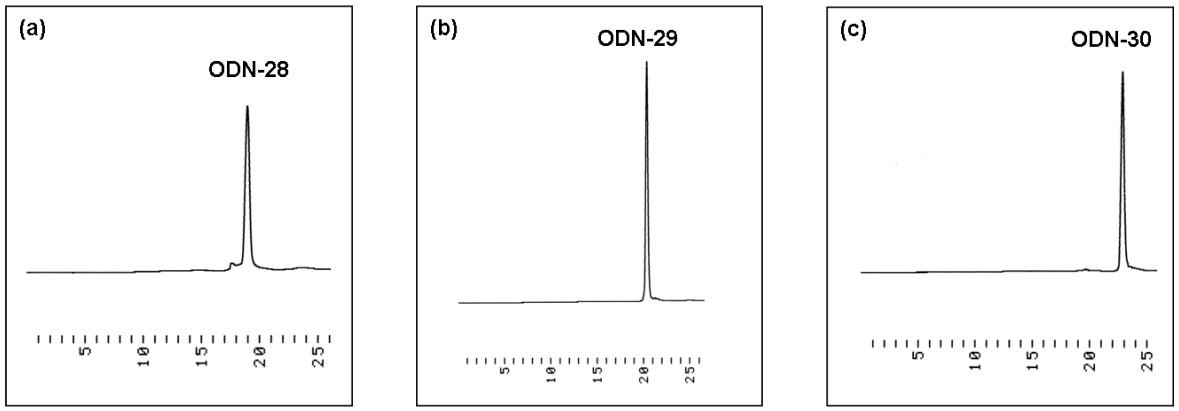

Figure S8. Reversed-phase HPLC profiles of purified single-stranded oligonucleotides containing 7-phenyl-7-deaza-2'-deoxyguanosine determined at 260 nm, (a) ODN-**28**; (b) ODN-**29**; (c) ODN-**30**. For elution the following solvent system was used: (A) MeCN and (B) 0.1 M (Et_3NH)OAc (pH 7.0): MeCN (95:5). Gradient II: 0-20 min 0-20% A in B, 20-25 min 20% A in B, flow rate 0.8 mL/min. X-axis corresponds to retention time [min] and y-axis corresponds to UV absorbance at 260 nm.

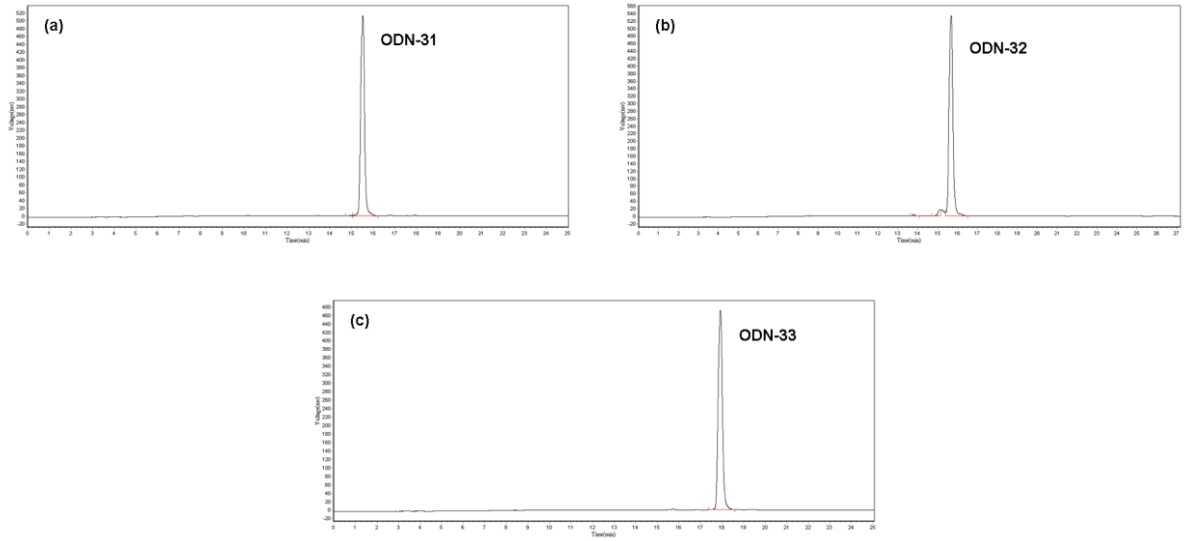

Figure S9. Reversed-phase HPLC profiles of purified single-stranded oligonucleotides containing 7-phenyltriazolyl-7-deaza-2'-deoxyguanosine determined at 260 nm, (a) ODN-**31**; (b) ODN-**32**; (c) ODN-**33**. For elution the following solvent system was used: (A) MeCN and (B) 0.1 M (Et_3NH)OAc (pH 7.0): MeCN (95:5). Gradient II: 0-20 min 0-20% A in B, 20-25 min 20% A in B, flow rate 0.8 mL/min. X-axis corresponds to retention time [min] and y-axis corresponds to UV absorbance at 260 nm, measured in mV.

Antiparallel Duplexes Containing 7-Deaza-2'-deoxyguanosine (1)

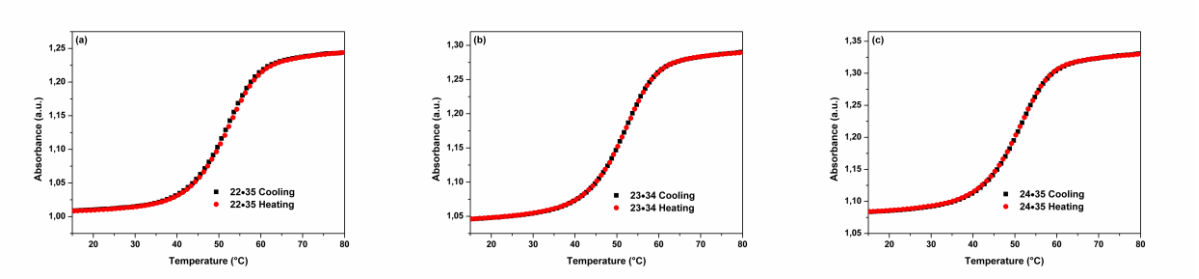

Figure S10. Thermal denaturation curves obtained from heating (red) and cooling (black) experiments monitored at 260 nm. (a) Duplex **22•35**; (b) duplex **23•34**; (c) duplex **24•35**. All the experiments were performed with 5 μM duplex concentrations at a heating rate of 1.0 °C/min in 1 M NaCl, 100 mM $MgCl_2$, 60 mM Na-cacodylate (pH 7) buffer.

Parallel Duplexes Containing 7-Deaza-2'-deoxyguanosine (1)

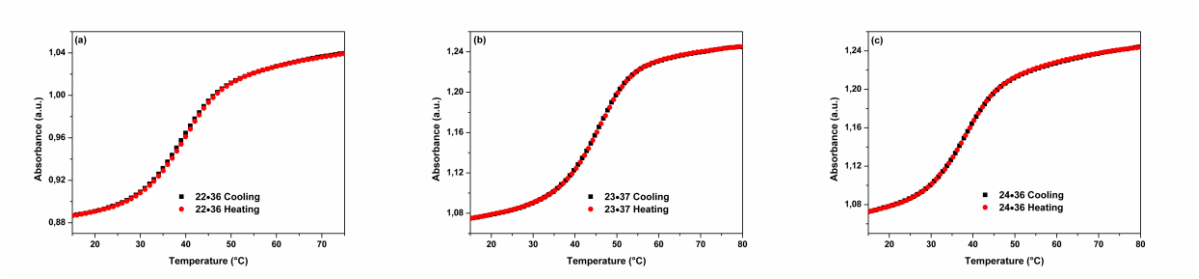

Figure S11. Thermal denaturation curves obtained from heating (red) and cooling (black) experiments monitored at 260 nm. (a) Duplex **22•36**; (b) duplex **23•37**; (c) duplex **24•36**.

DNA-RNA Hybrids Containing 7-Deaza-2'-deoxyguanosine (1)

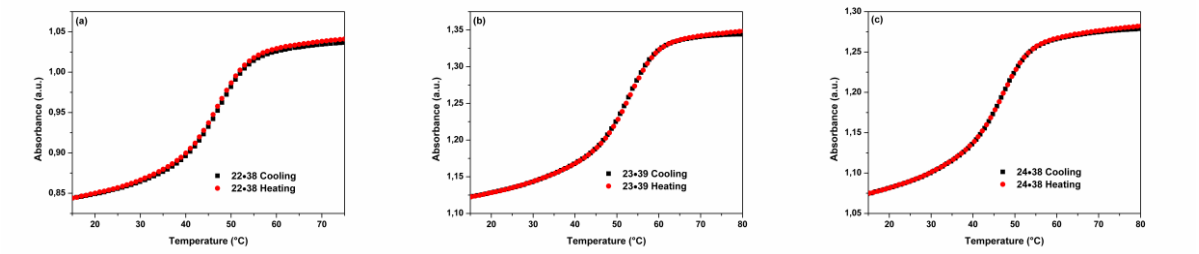

Figure S12. Thermal denaturation curves obtained from heating (red) and cooling (black) experiments monitored at 260 nm. (a) Duplex **22•38**; (b) duplex **23•39**; (c) duplex **24•38**.

Antiparallel Duplexes Containing 8-Phenyl-7-deaza-2'-deoxyguanosine (2)

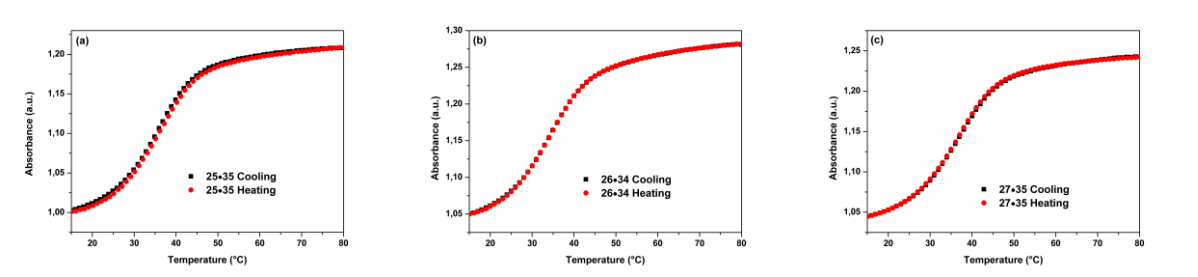

Figure S13. Thermal denaturation curves obtained from heating (red) and cooling (black) experiments monitored at 260 nm. (a) Duplex **25•35**; (b) duplex **26•34**; (c) duplex **27•35**. All the experiments were performed with 5 μM duplex concentrations at a heating rate of 1.0 °C/min in 1 M NaCl, 100 mM $MgCl_2$, 60 mM Na-cacodylate (pH 7) buffer.

Parallel Duplexes Containing 8-Phenyl-7-deaza-2'-deoxyguanosine (2)

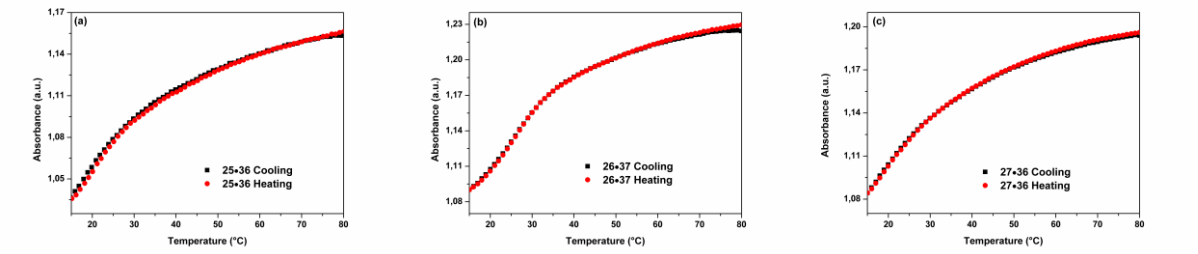

Figure S14. Thermal denaturation curves obtained from heating (red) and cooling (black) experiments monitored at 260 nm. (a) Duplex **25•36**; (b) duplex **26•37**; (c) duplex **27•36**.

DNA-RNA Hybrids Containing 8-Phenyl-7-deaza-2'-deoxyguanosine (2)

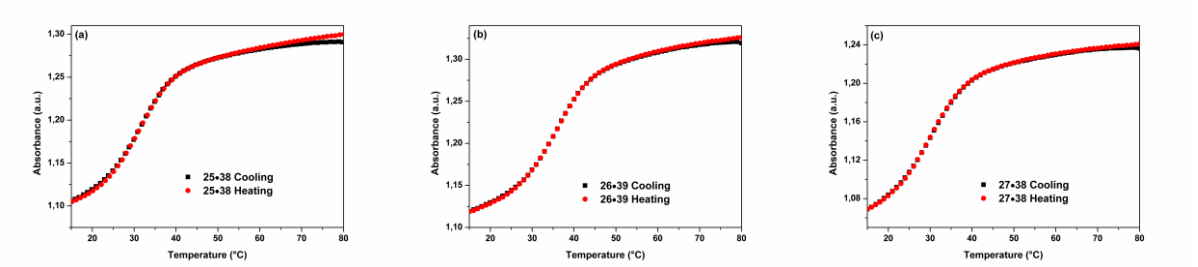

Figure S15. Thermal denaturation curves obtained from heating (red) and cooling (black) experiments monitored at 260 nm. (a) Duplex **25•38**; (b) duplex **26•39**; (c) duplex **27•38**.

Antiparallel Duplexes Containing 7-Phenyl-7-deaza-2'-deoxyguanosine (3)

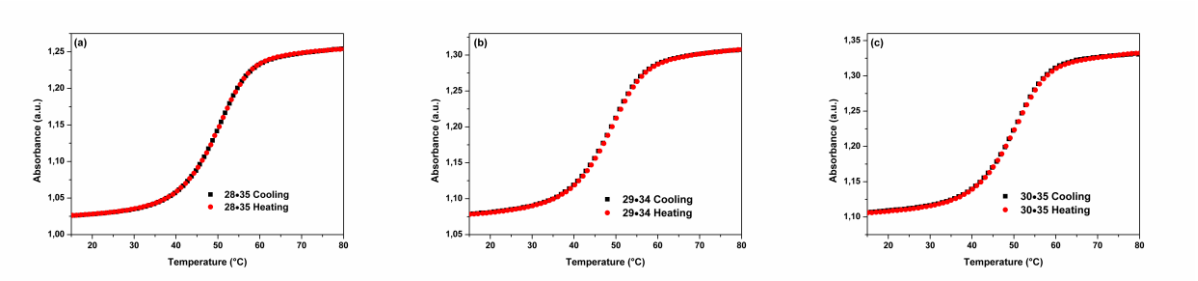

Figure S16. Thermal denaturation curves obtained from heating (red) and cooling (black) experiments monitored at 260 nm. (a) Duplex **28•35**; (b) duplex **29•34**; (c) duplex **30•35**. All the experiments were performed with 5 μM duplex concentrations at a heating rate of 1.0 °C/min in 1 M NaCl, 100 mM $MgCl_2$, 60 mM Na-cacodylate (pH 7) buffer.

Parallel Duplexes Containing 7-Phenyl-7-deaza-2'-deoxyguanosine (3)

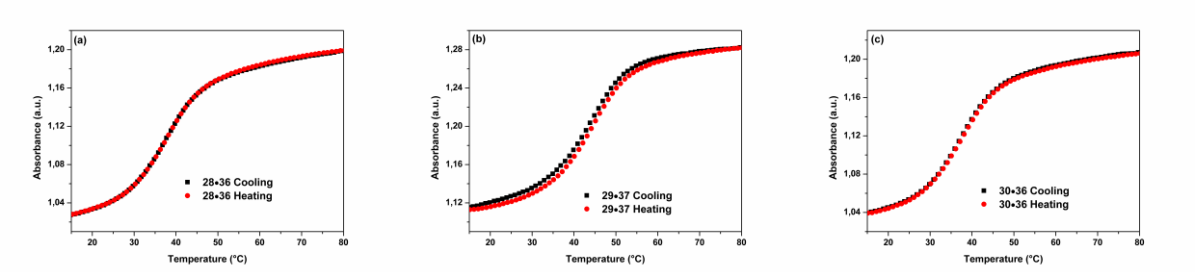

Figure S17. Thermal denaturation curves obtained from heating (red) and cooling (black) experiments monitored at 260 nm. (a) Duplex **28•36**; (b) duplex **29•37**; (c) duplex **30•36**.

DNA-RNA Hybrids Containing 7-Phenyl-7-deaza-2'-deoxyguanosine (3)

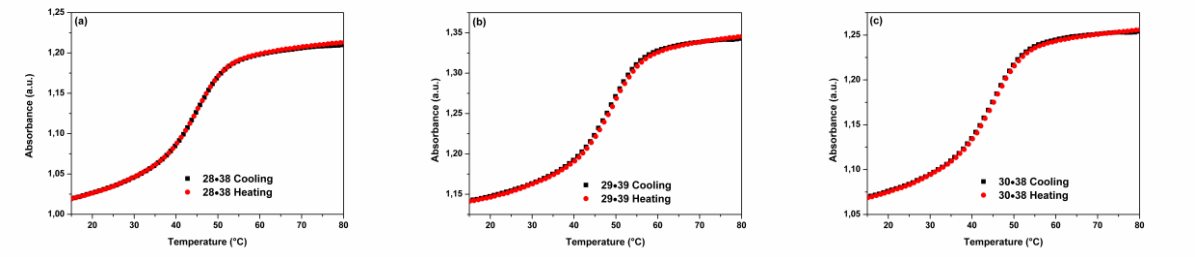

Figure S18. Thermal denaturation curves obtained from heating (red) and cooling (black) experiments monitored at 260 nm. (a) Duplex **28•38**; (b) duplex **29•39**; (c) duplex **30•38**.

Antiparallel Duplexes Containing 7-Phenyltriazolyl-7-deaza-2'-deoxyguanosine (4)

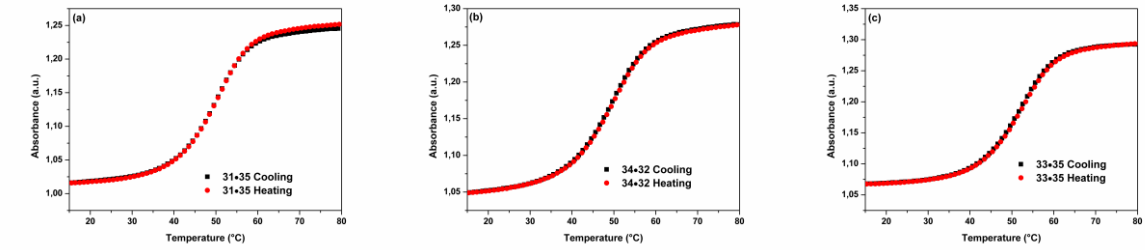

Figure S19. Thermal denaturation curves obtained from heating (red) and cooling (black) experiments monitored at 260 nm. (a) Duplex **31•35**; (b) duplex **32•34**; (c) duplex **33•35**. All the experiments were performed with 5 μM duplex concentrations at a heating rate of 1.0 °C/min in 1 M NaCl, 100 mM $MgCl_2$, 60 mM Na-cacodylate (pH 7) buffer.

Parallel Duplexes Containing 7-Phenyltriazolyl-7-deaza-2'-deoxyguanosine (4)

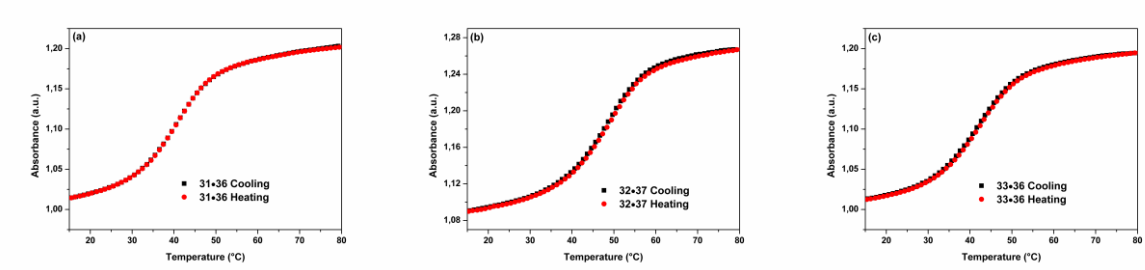

Figure S20. Thermal denaturation curves obtained from heating (red) and cooling (black) experiments monitored at 260 nm. (a) Duplex **31•36**; (b) duplex **32•37**; (c) duplex **33•36**.

DNA-RNA Hybrids Containing 7-Phenyltriazolyl-7-deaza-2'-deoxyguanosine (4)

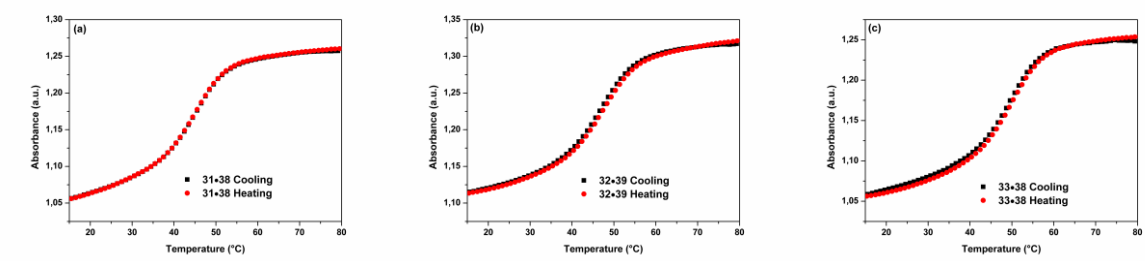

Figure S21. Thermal denaturation curves obtained from heating (red) and cooling (black) experiments monitored at 260 nm. (a) Duplex **31•38**; (b) duplex **32•39**; (c) duplex **33•38**.

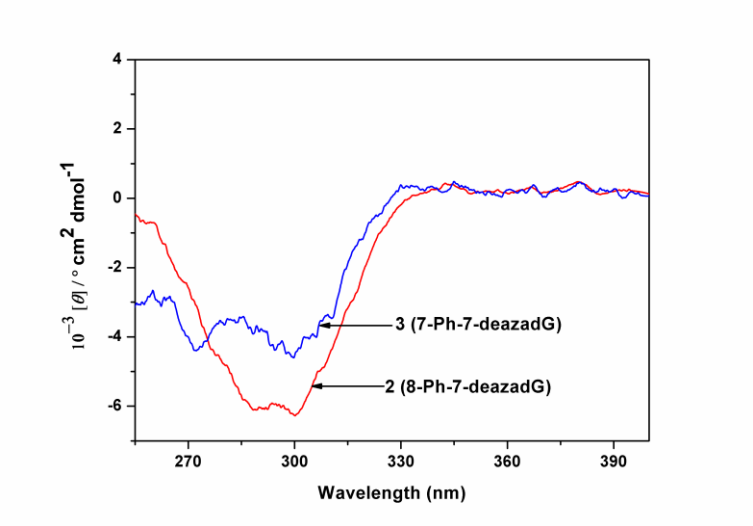

Figure S22. CD spectra of nucleosides **2-3**. Measurements were performed in 1 M NaCl, 100 mM $MgCl_2$, and 60 mM Na-cacodylate (pH 7.0) at 5 °C.

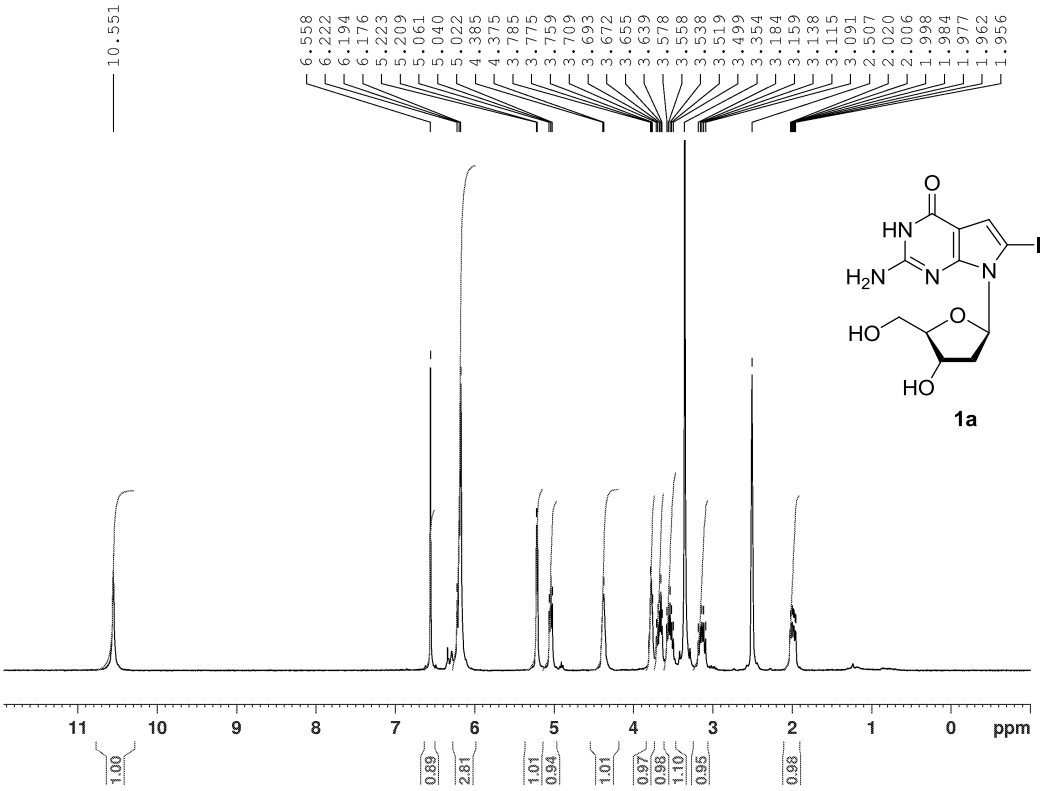

Figure 23. ^{1}H NMR spectrum of compound **1a**.

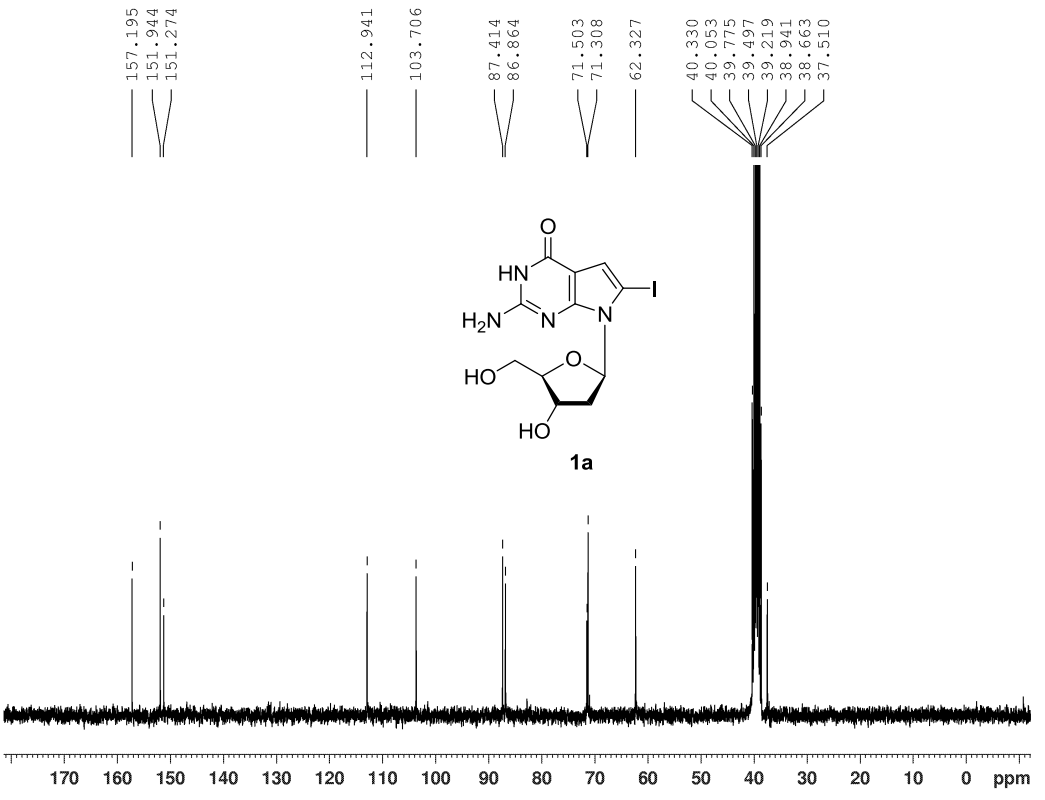

Figure 24. ^{13}C NMR spectrum of compound **1a**.

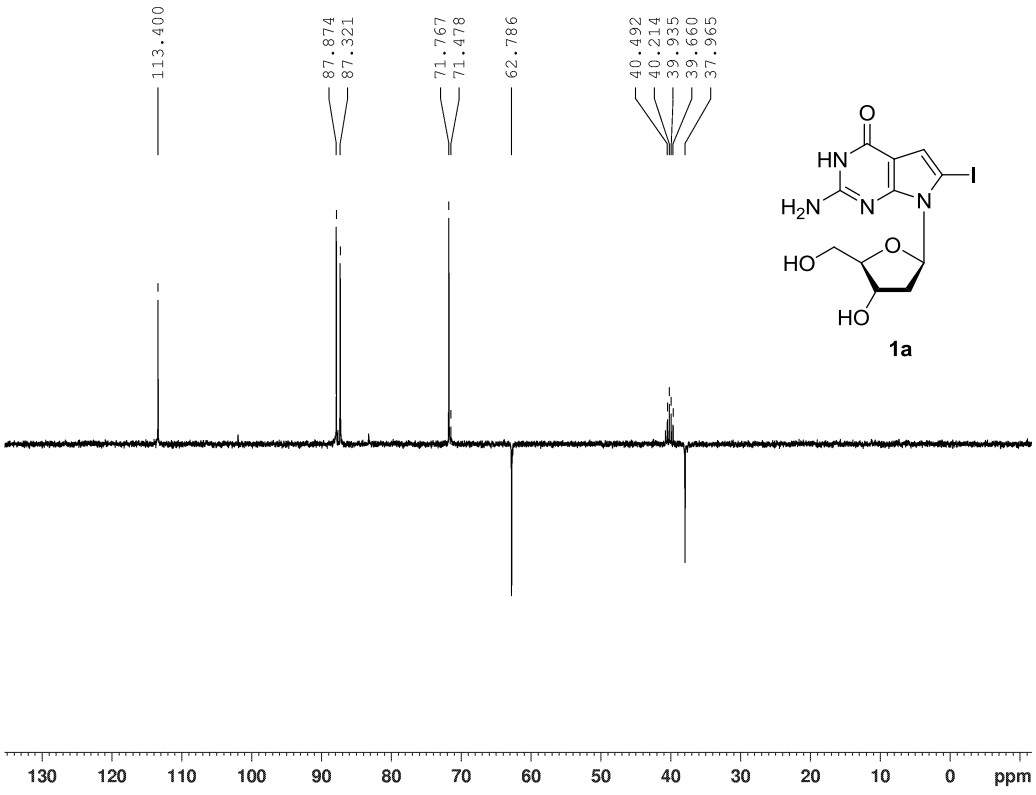

Figure 25. DEPT-135 NMR spectrum of compound **1a**.

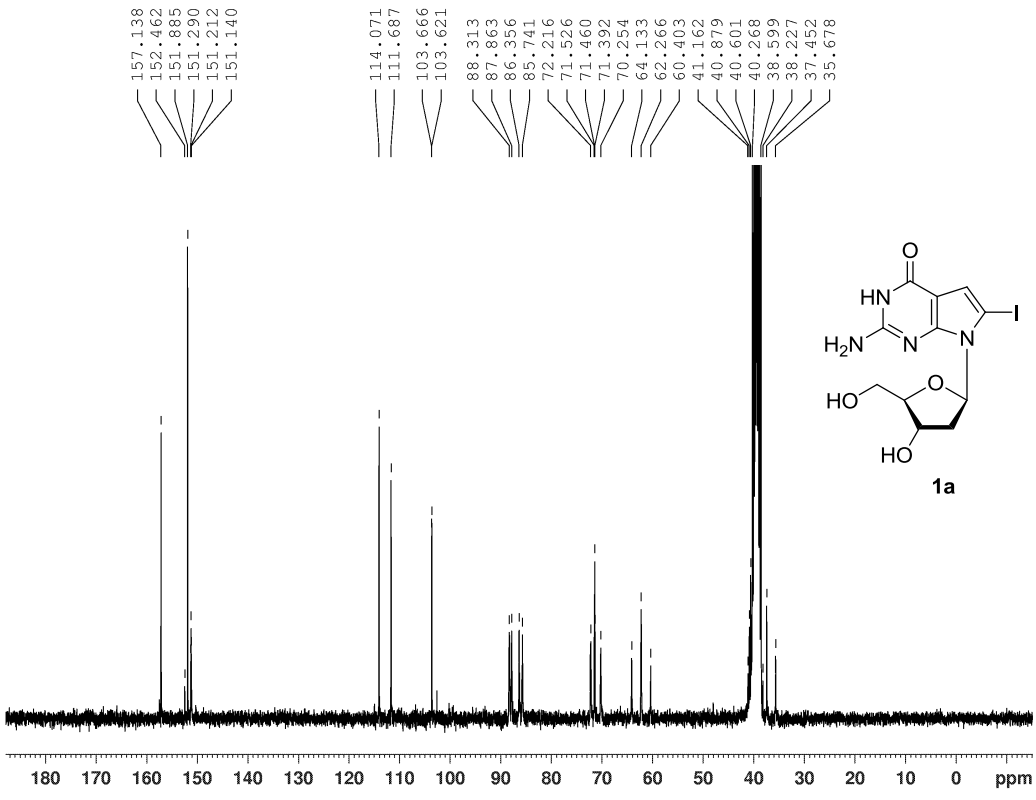

Figure 26. ^{1}H-^{13}C gated-decoupled NMR spectrum of compound **1a**.

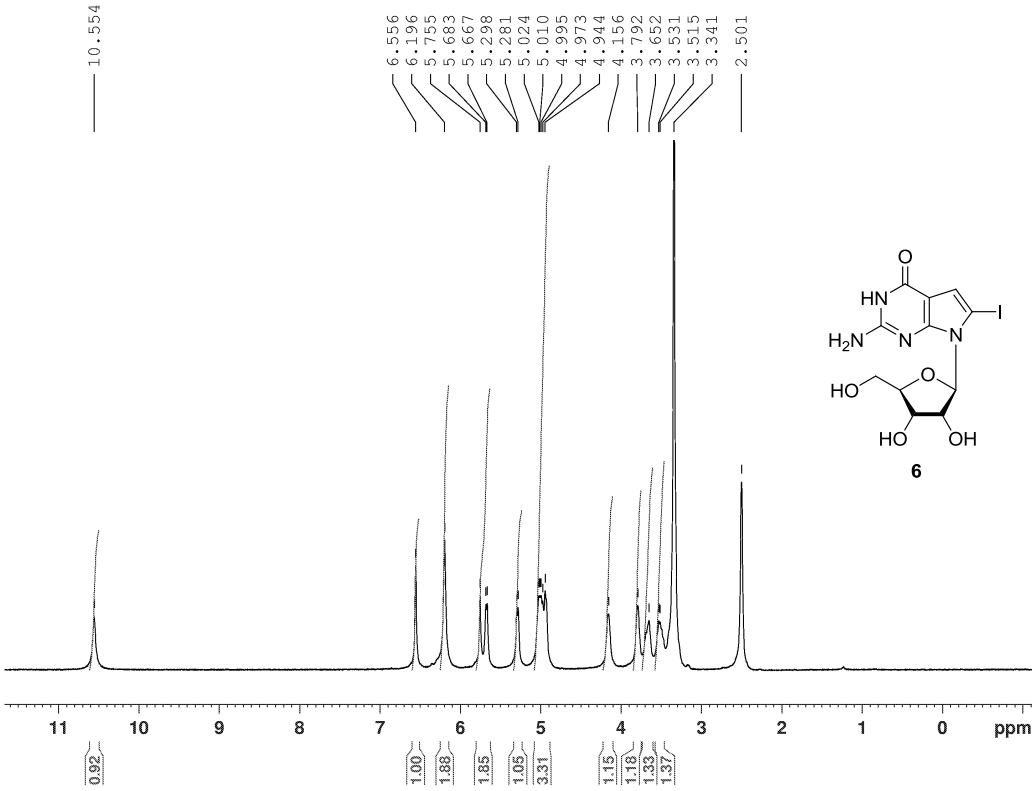

Figure 27. ^{1}H NMR spectrum of compound **6**.

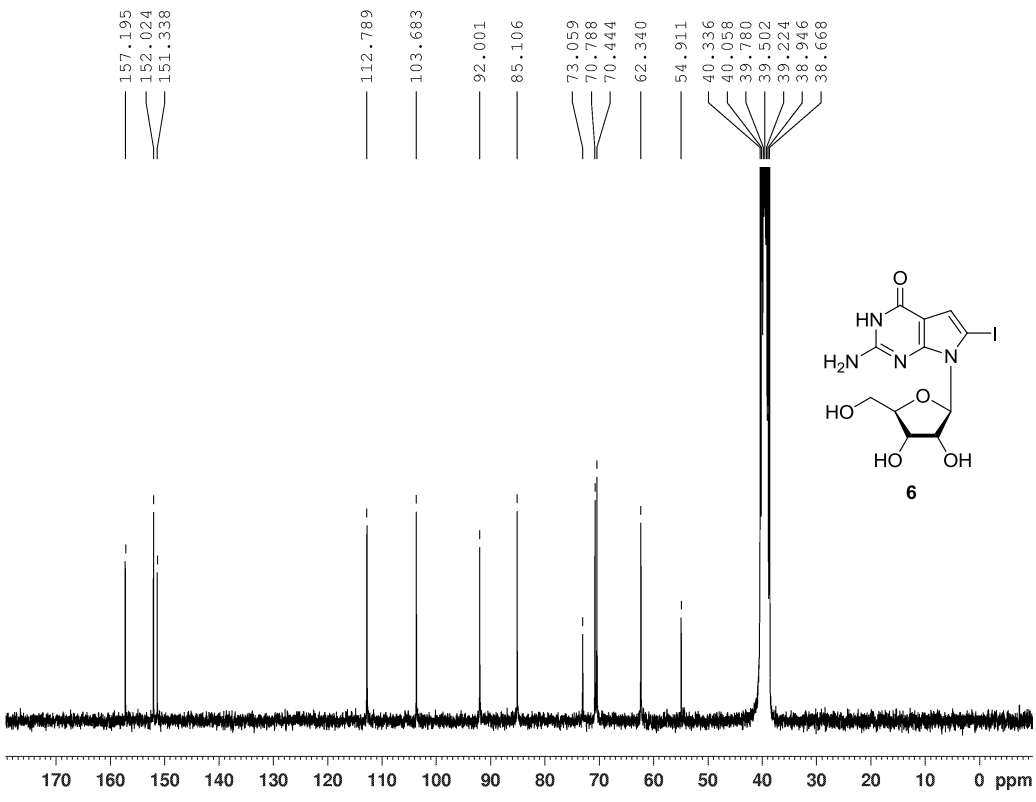

Figure 28. ^{13}C NMR spectrum of compound **6**.

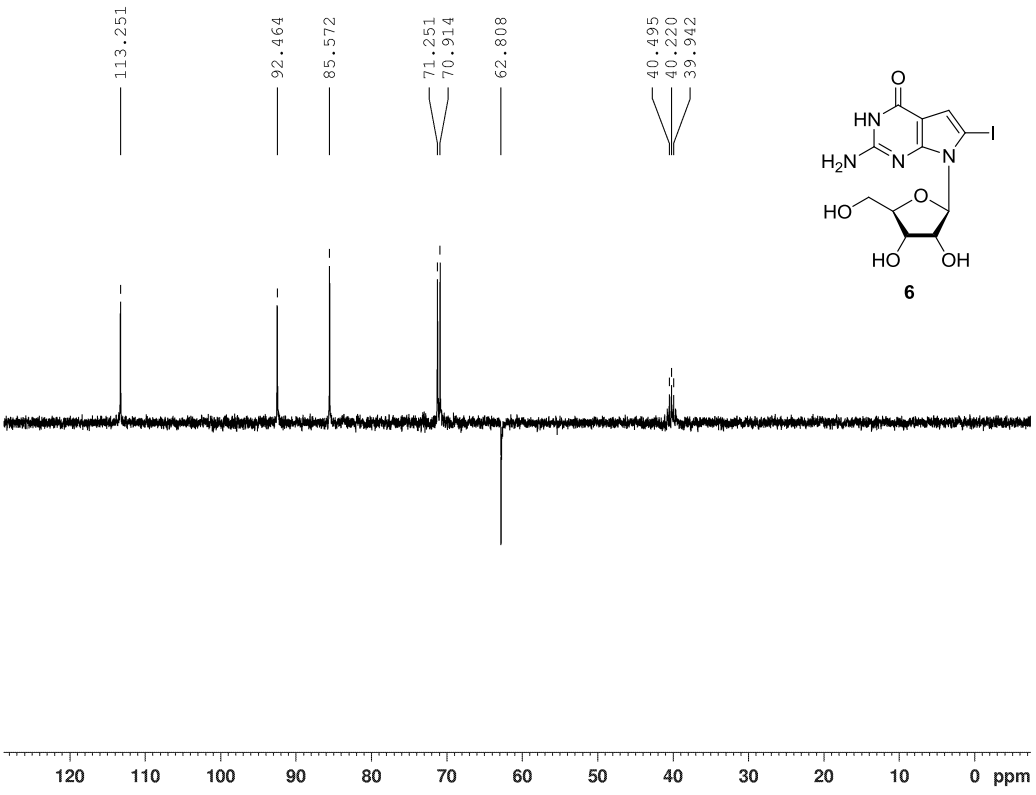

Figure 29. DEPT-135 NMR spectrum of compound **6**.

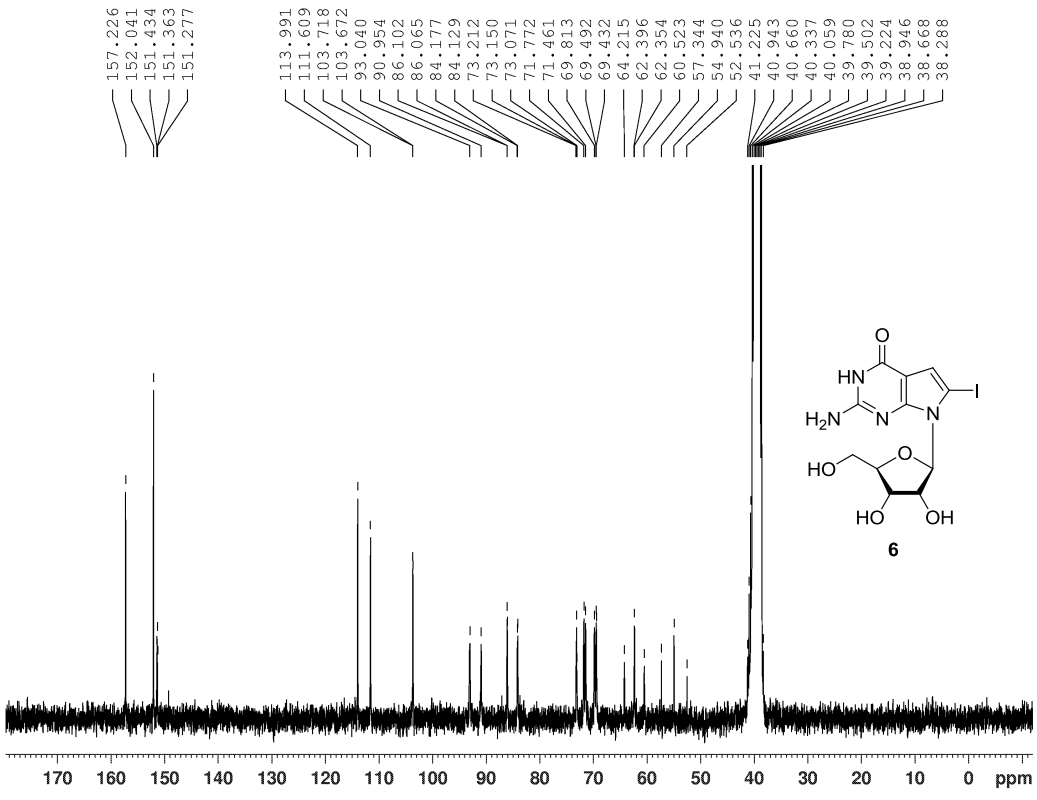

Figure 30. ^{1}H-^{13}C gated-decoupled NMR spectrum of compound **6**.

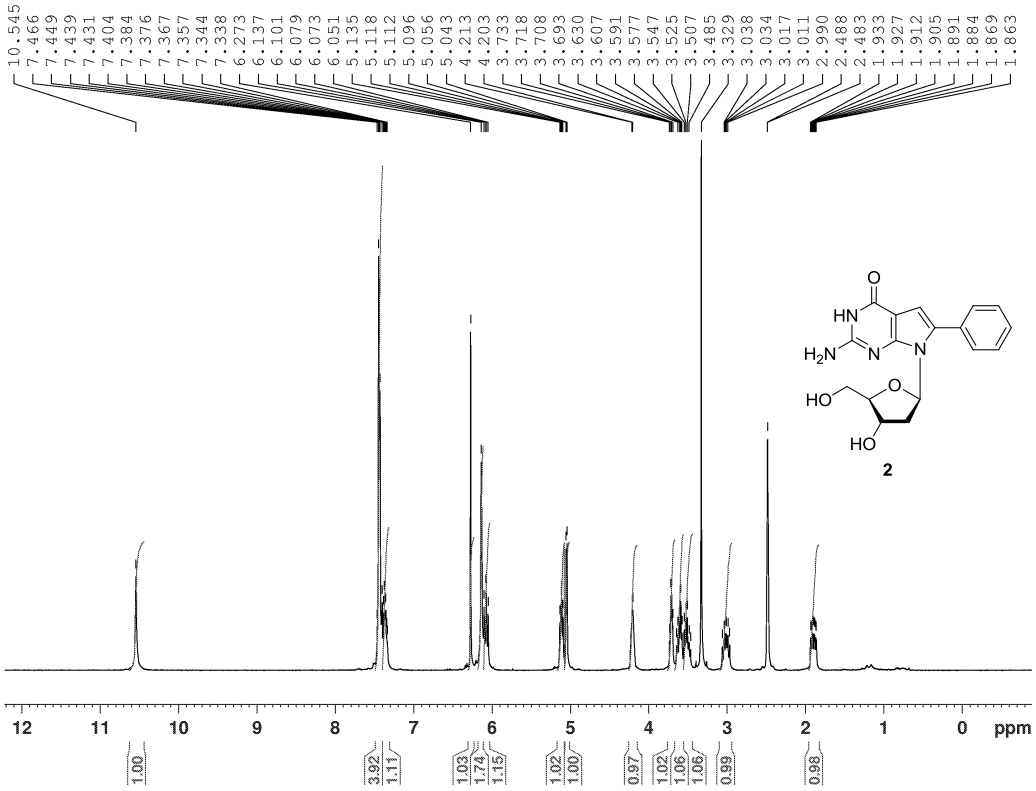

Figure 31. ^{1}H NMR spectrum of compound **2**.

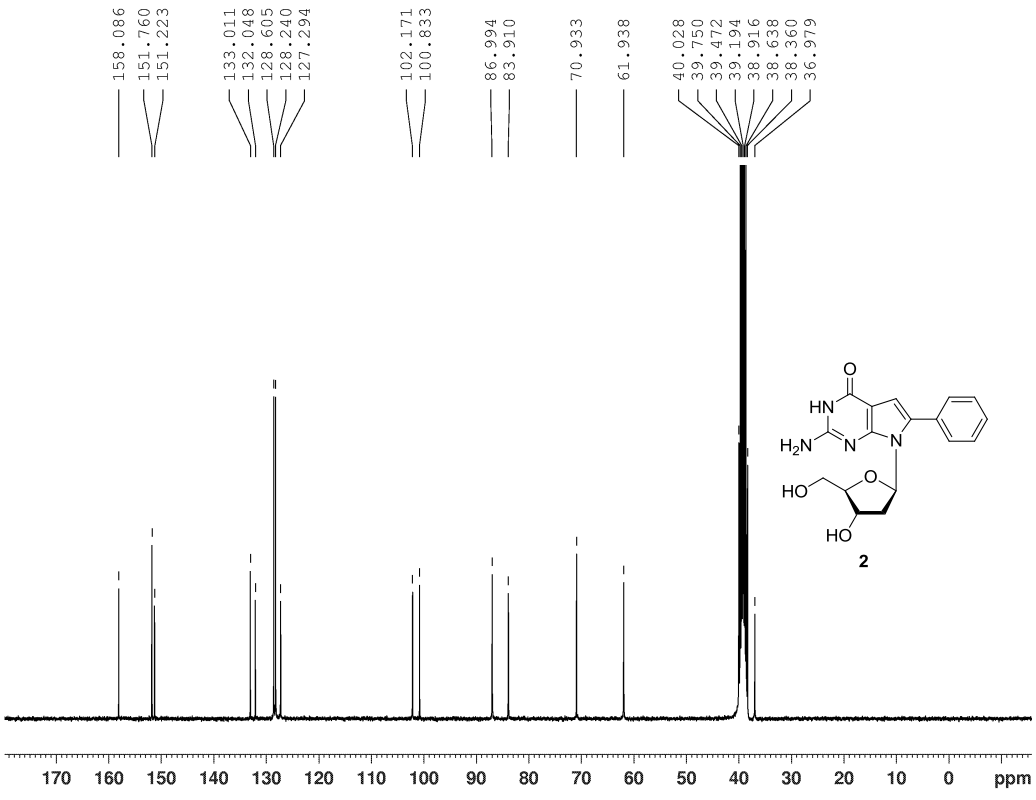

Figure 32. ^{13}C NMR spectrum of compound **2**.

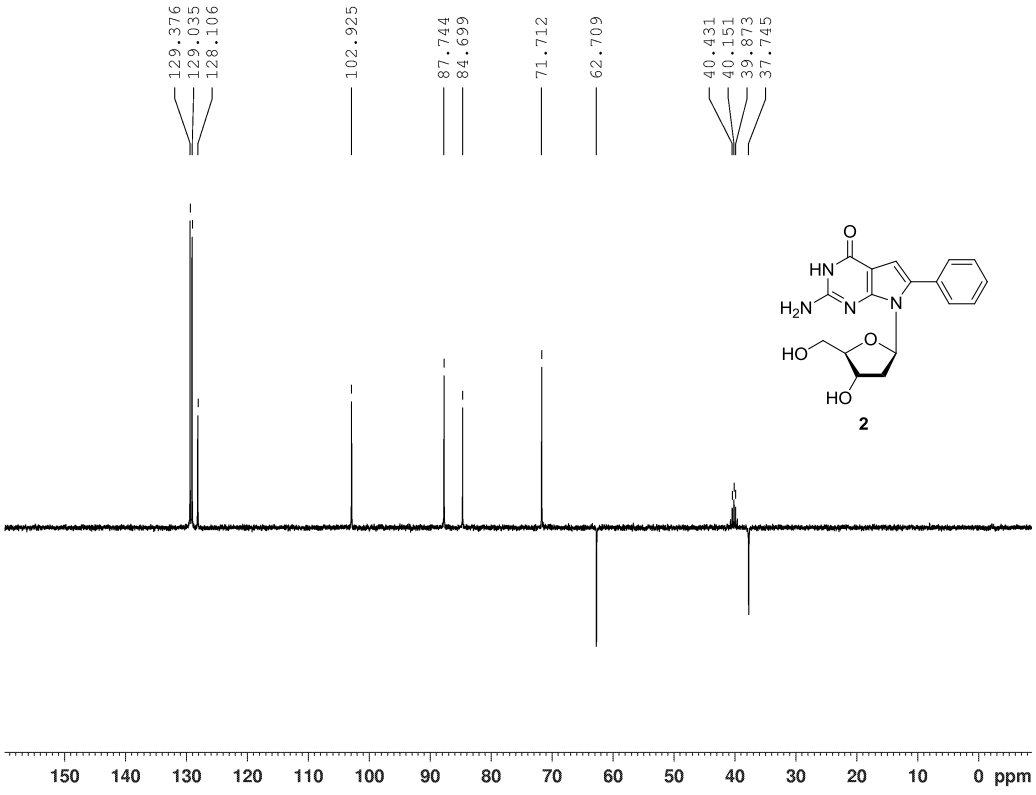

Figure 33. DEPT-135 NMR spectrum of compound **2.**

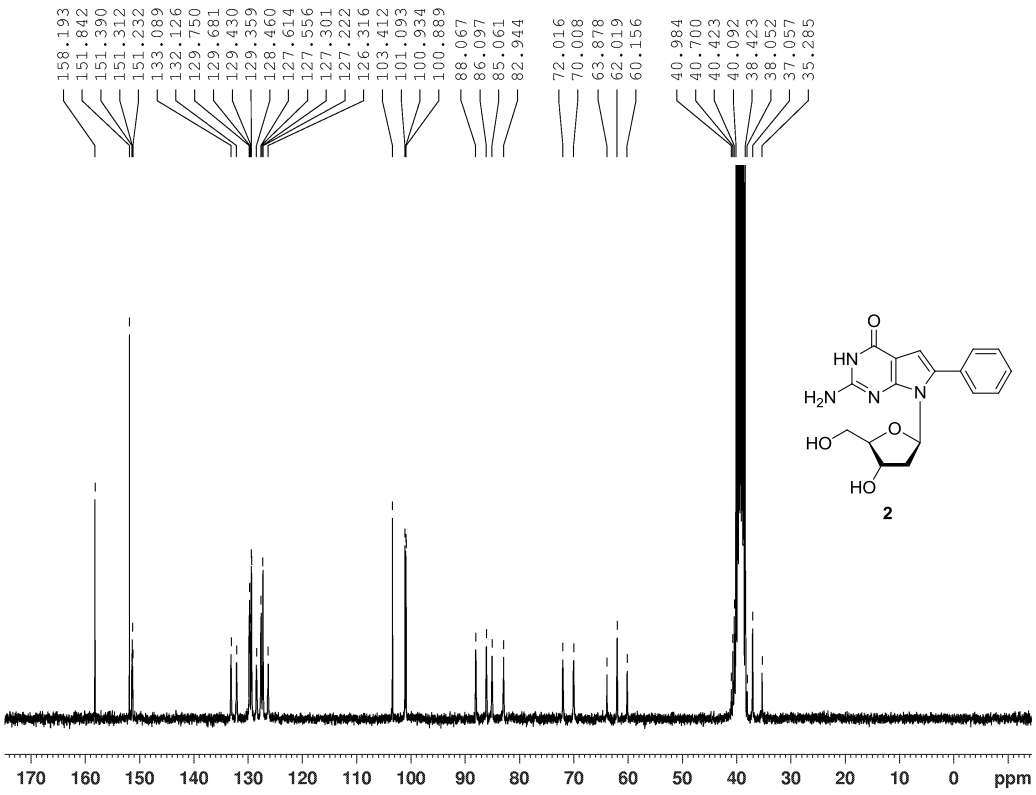

Figure 34. ^{1}H-^{13}C gated-decoupled NMR spectrum of compound **2.**

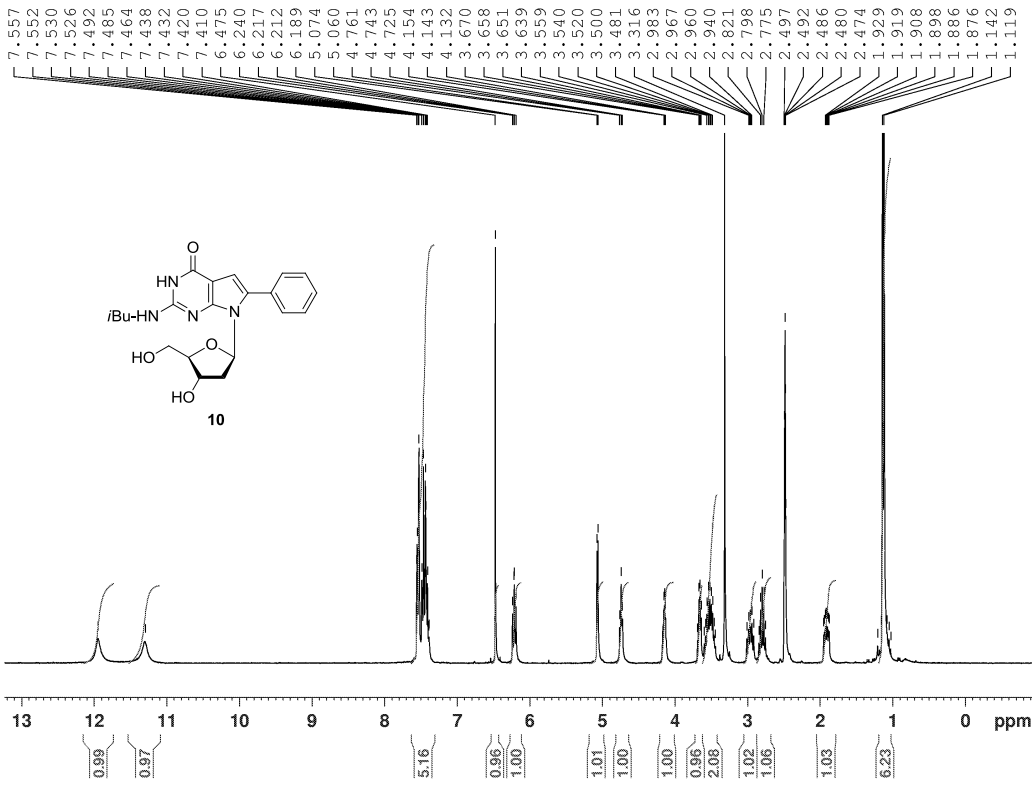

Figure 35. ^{1}H NMR spectrum of compound **10**.

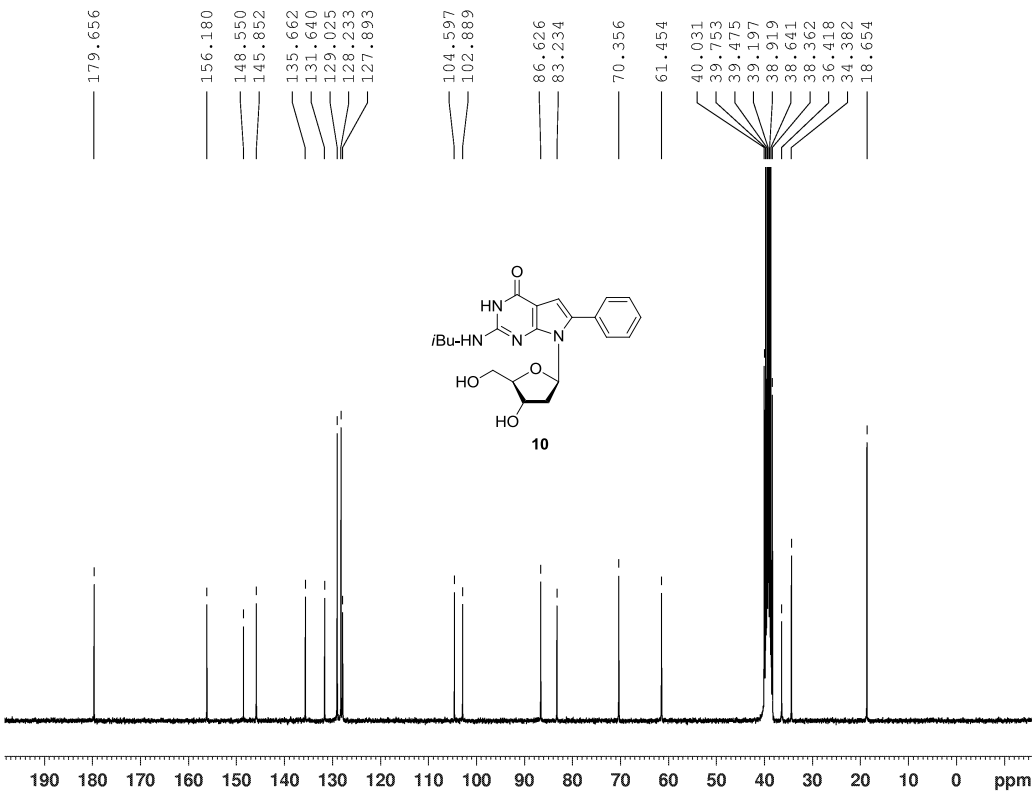

Figure 36. ^{13}C NMR spectrum of compound **10**.

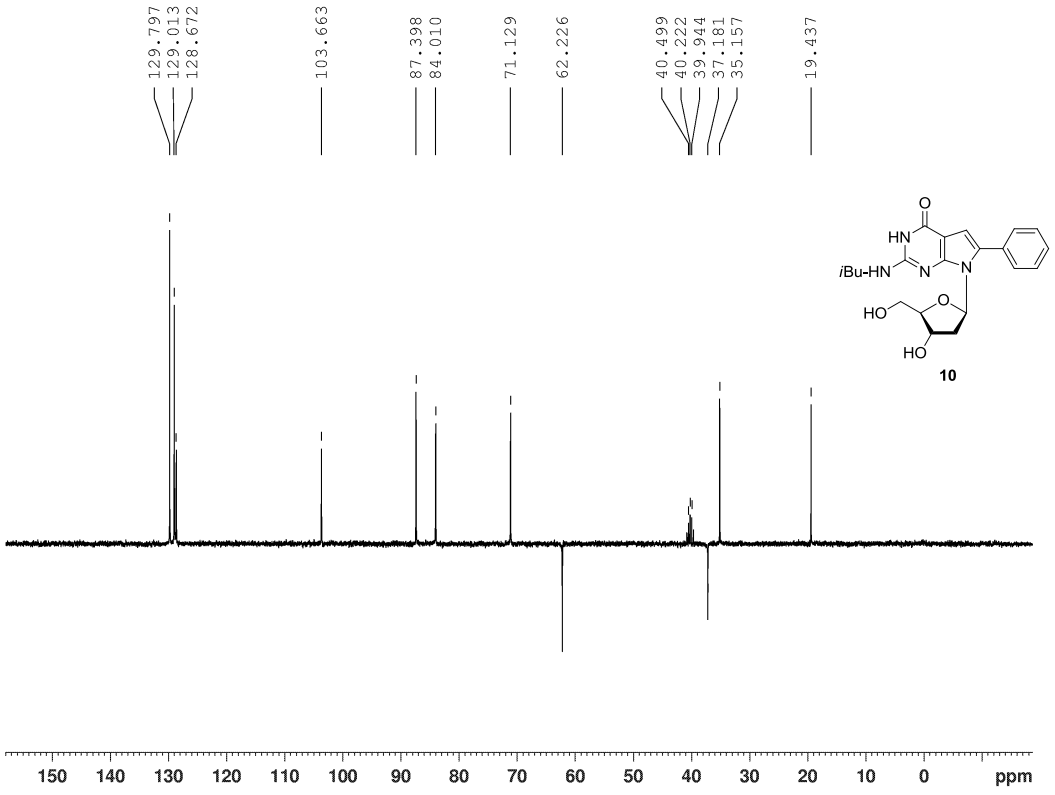

Figure 37. DEPT-135 NMR spectrum of compound **10**.

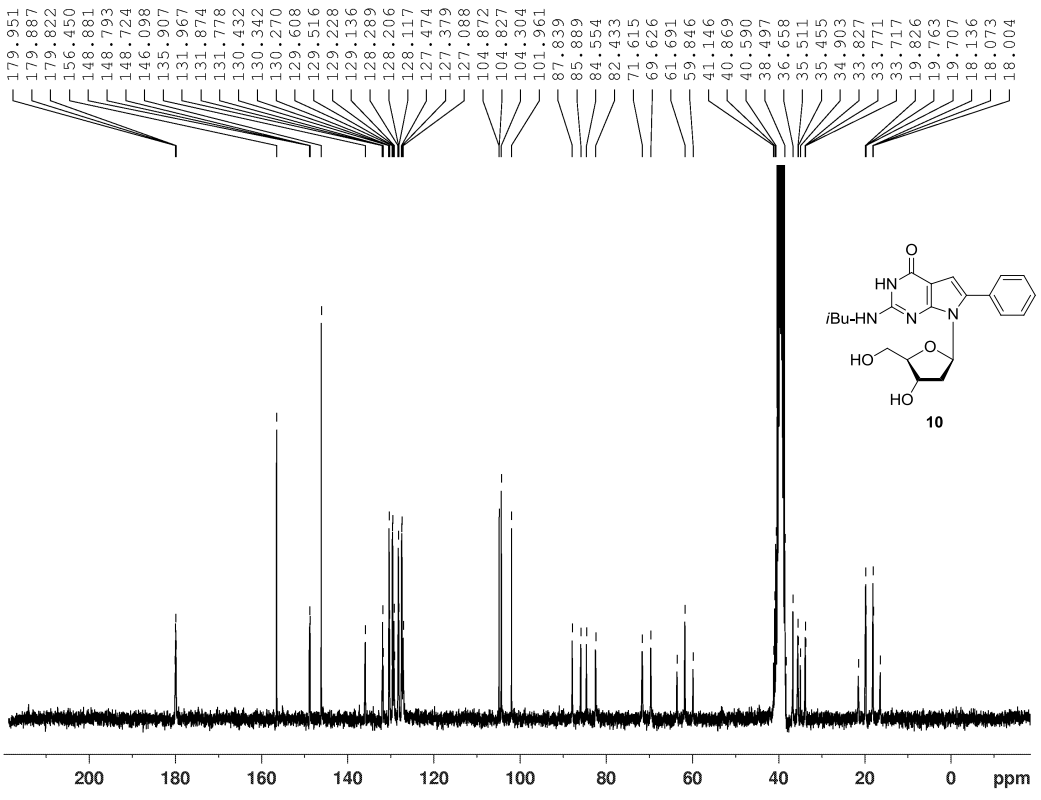

Figure 38. ^{1}H-^{13}C gated-decoupled NMR spectrum of compound **10**.

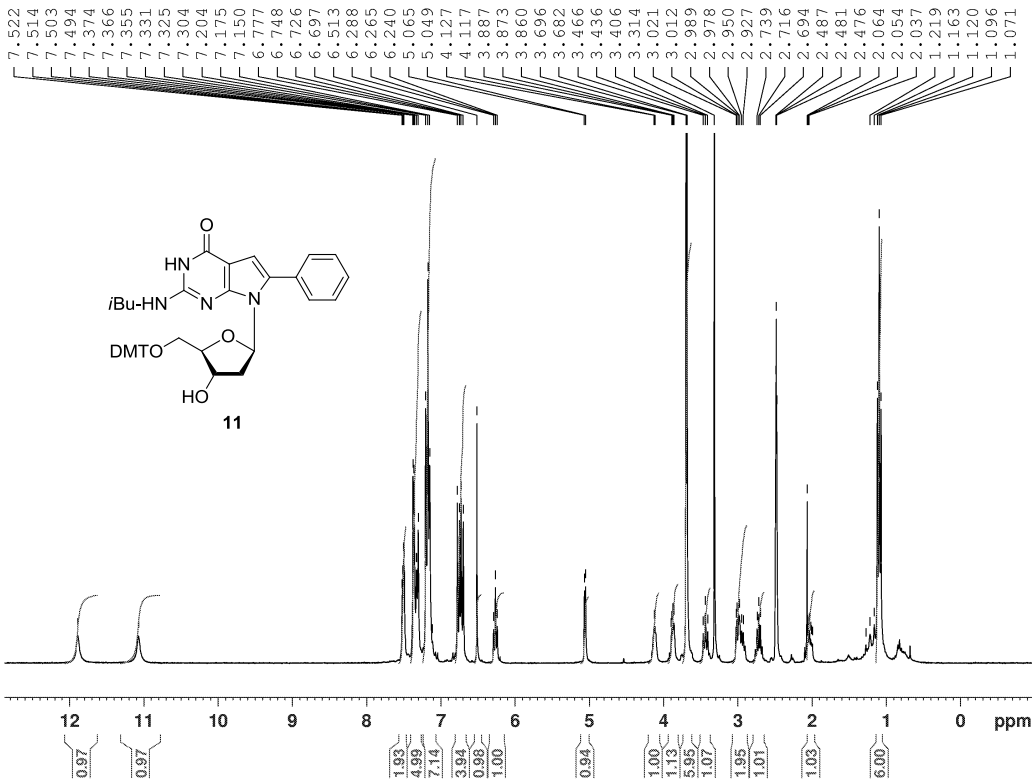

Figure 39. ^{1}H NMR spectrum of compound **11**.

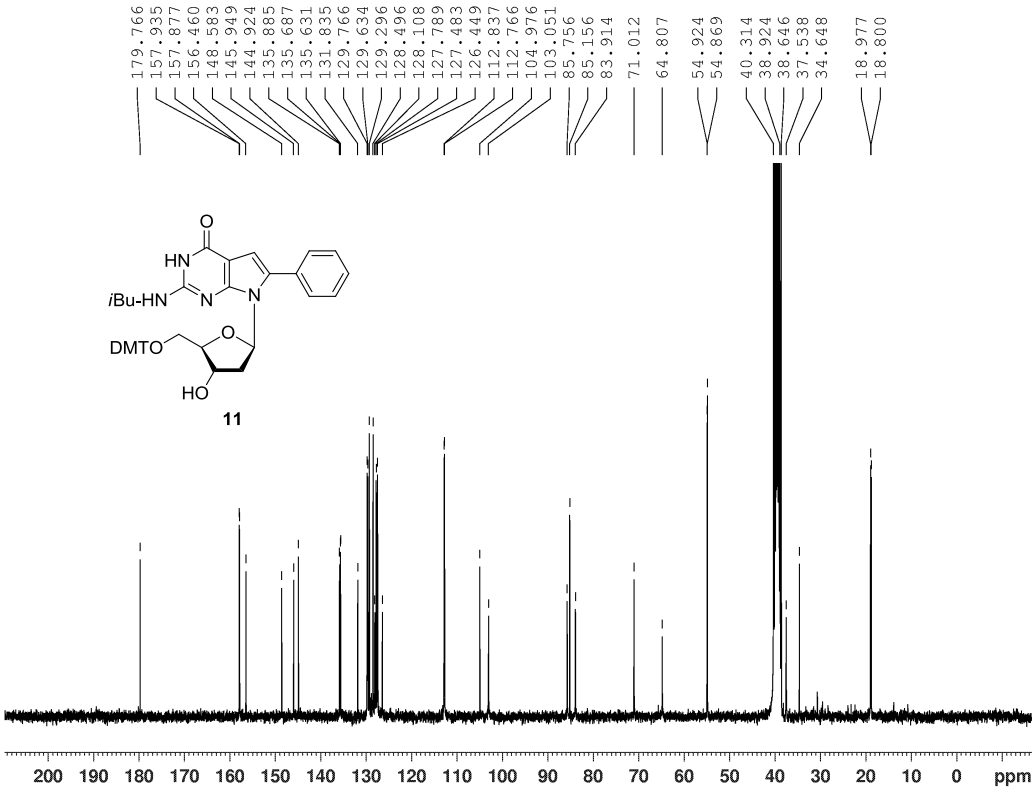

Figure 40. ^{13}C NMR spectrum of compound **11**.

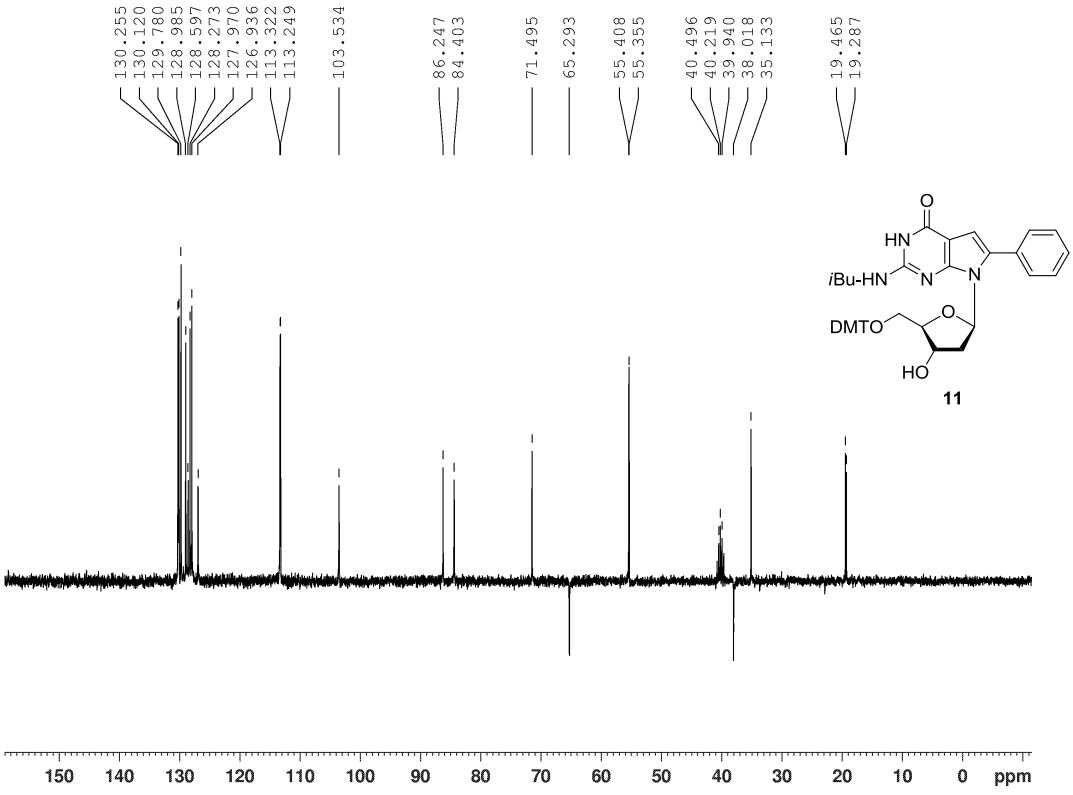

Figure 41. DEPT-135 NMR spectrum of compound **11**.

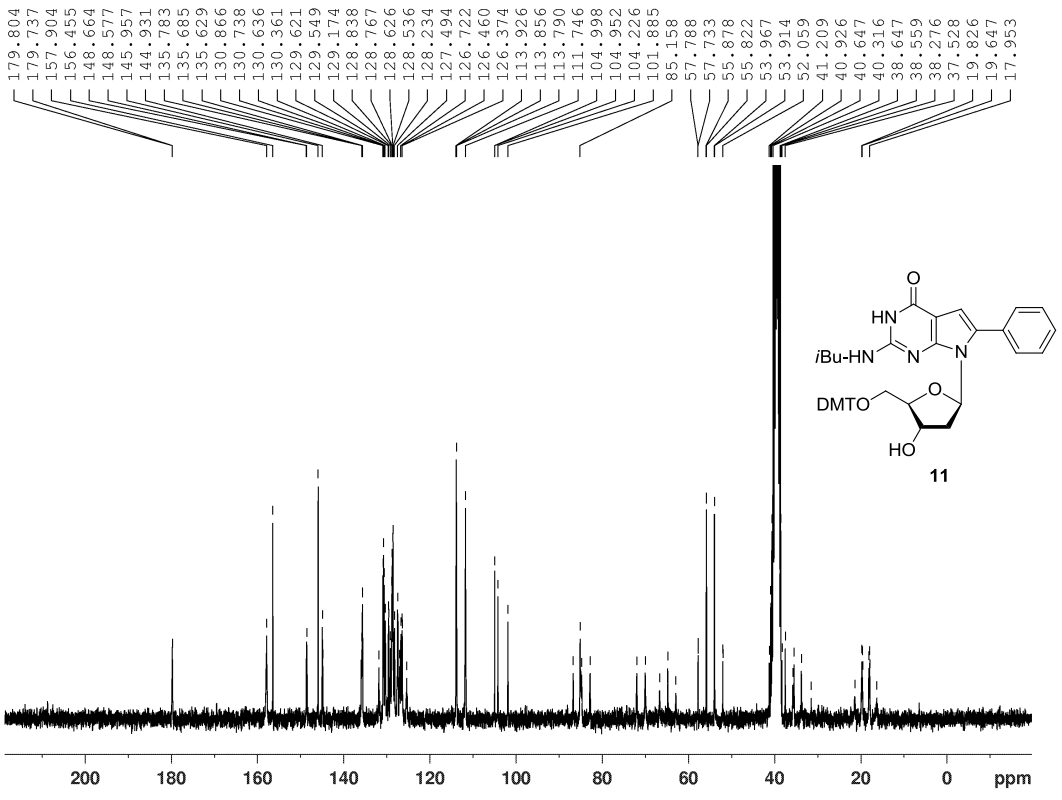

Figure 42. ^{1}H-^{13}C gated-decoupled NMR spectrum of compound **11**.

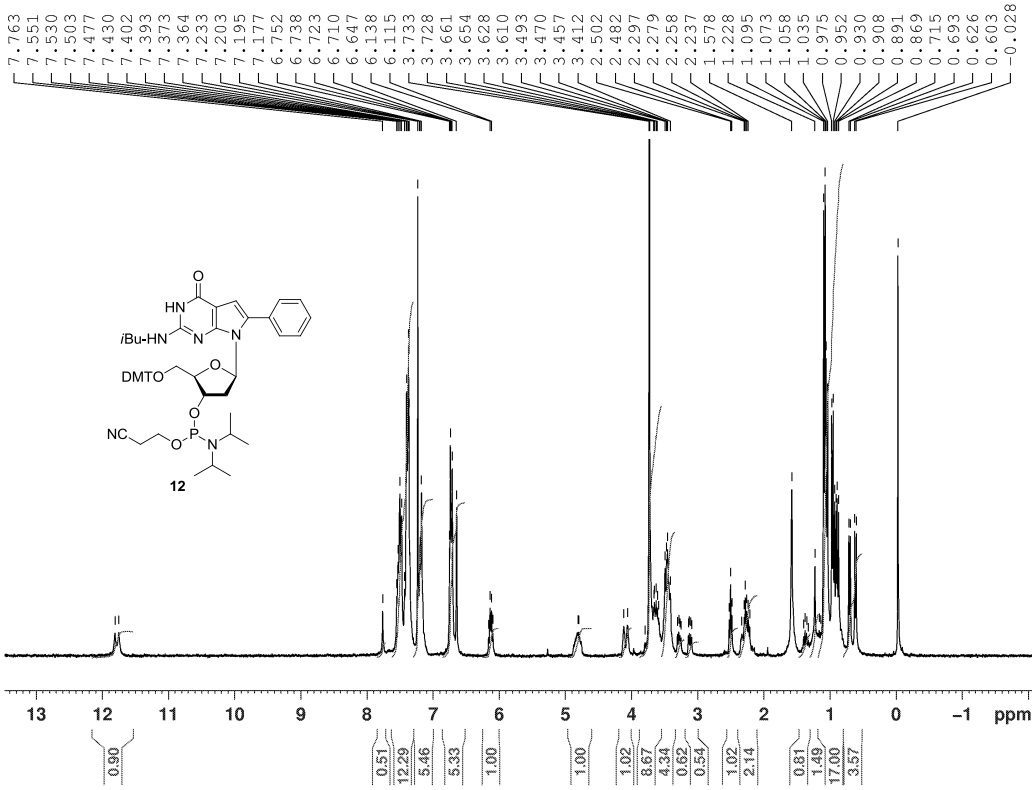

Figure 43. ^{1}H NMR spectrum of compound **12**.

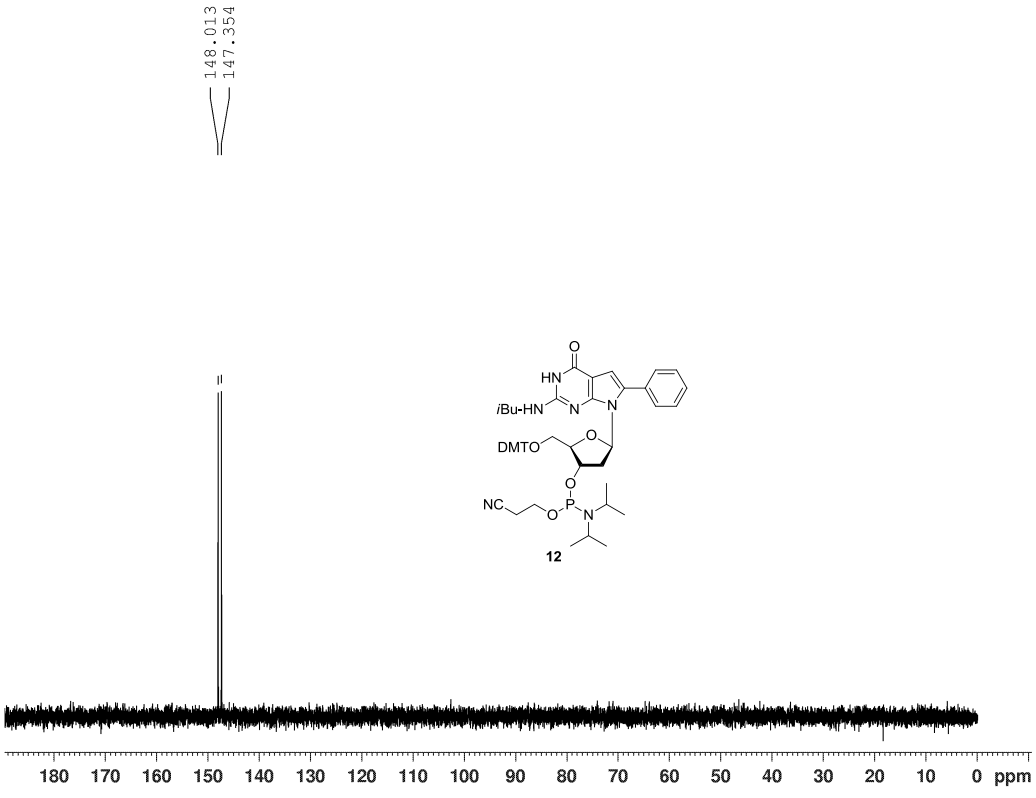

Figure 44. ^{31}P NMR spectrum of compound **12**.

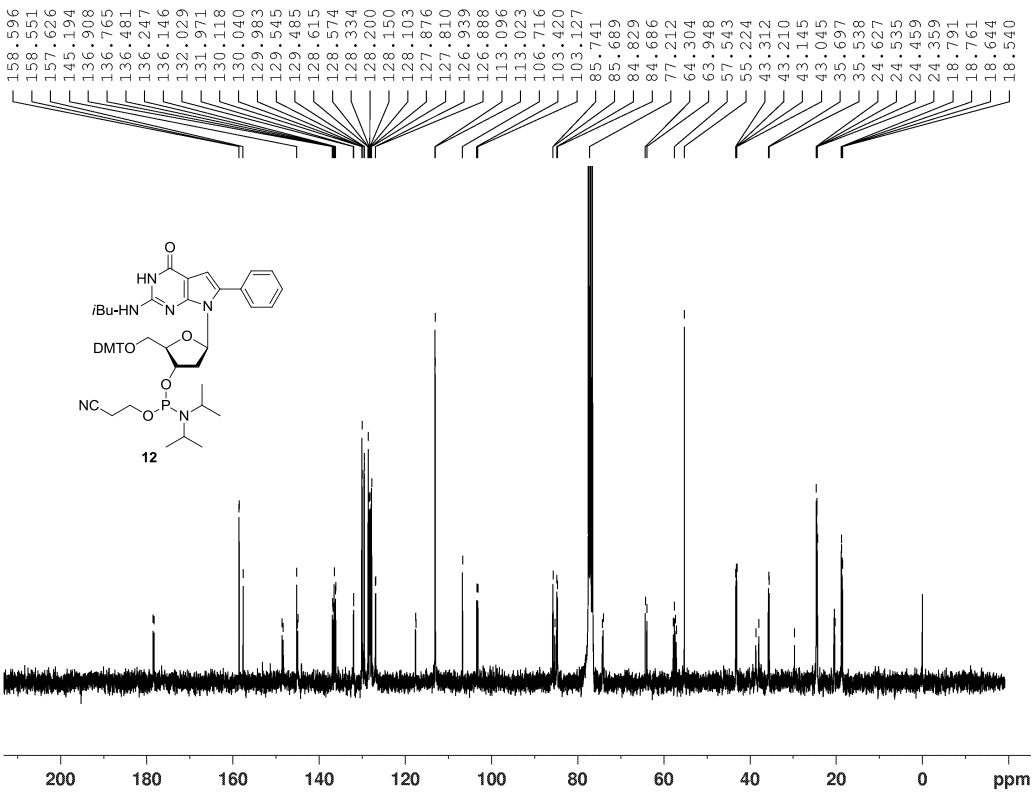

Figure 45. ^{13}C NMR spectrum of compound **12**.

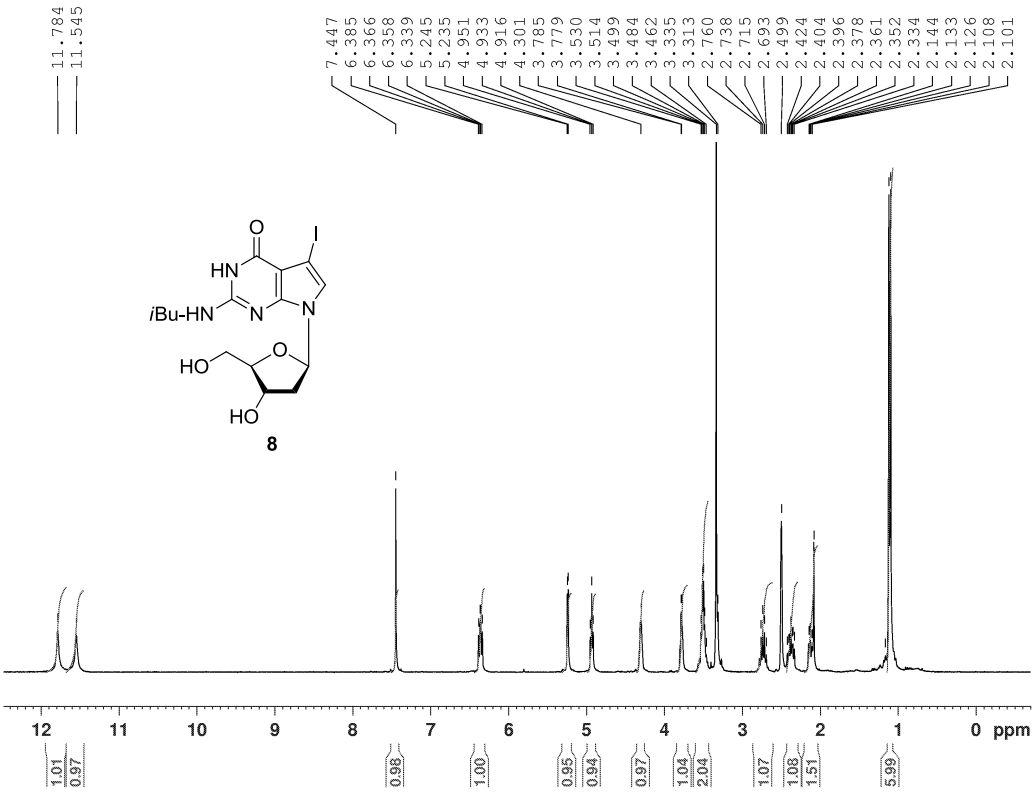

Figure 46. ^{1}H NMR spectrum of compound **8**.

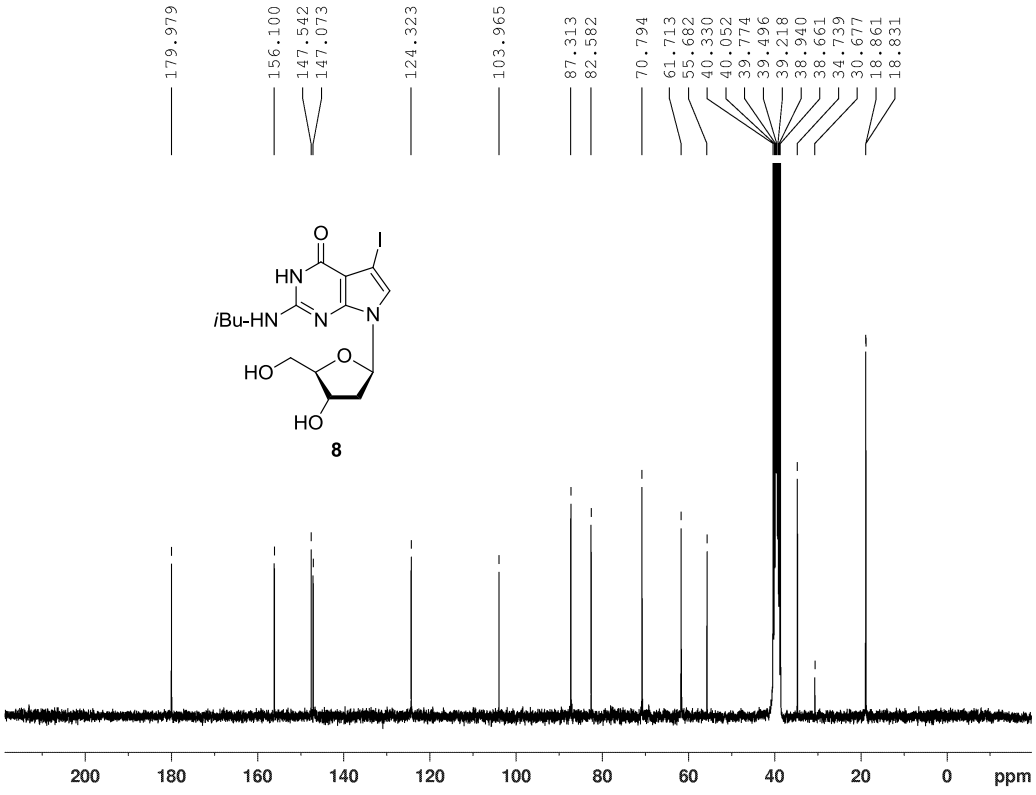

Figure 47. ^{13}C NMR spectrum of compound **8**.

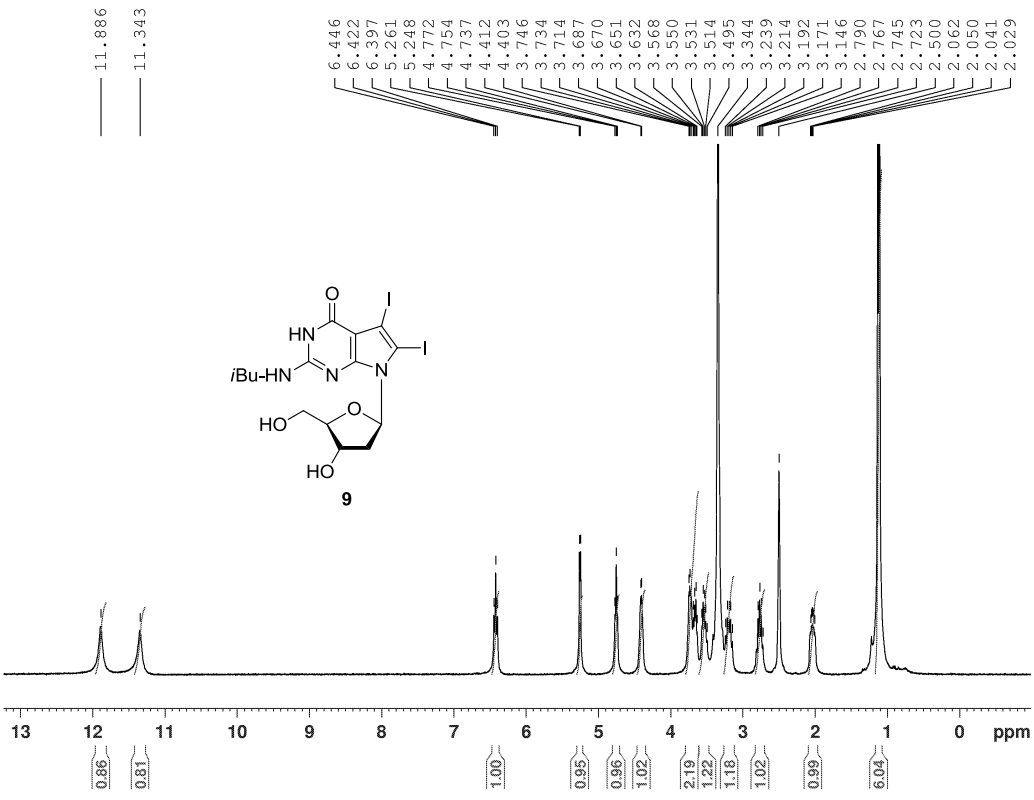

Figure 48. ^{1}H NMR spectrum of compound **9**.

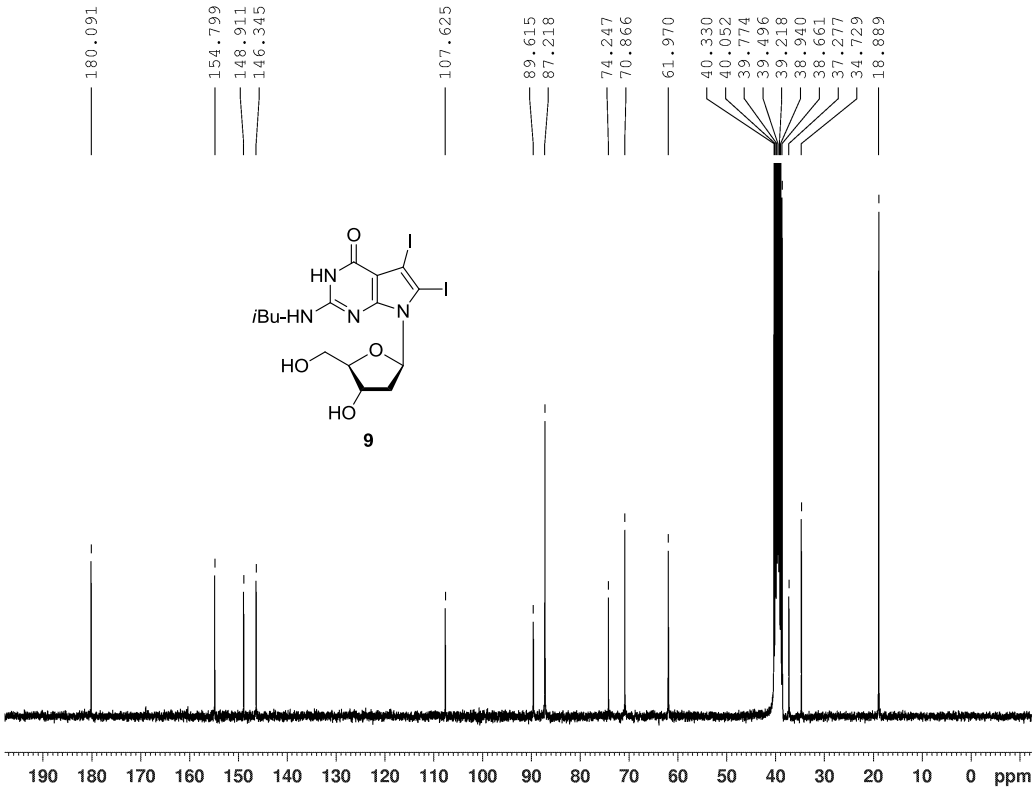

Figure 49. ^{13}C NMR spectrum of compound **9**.

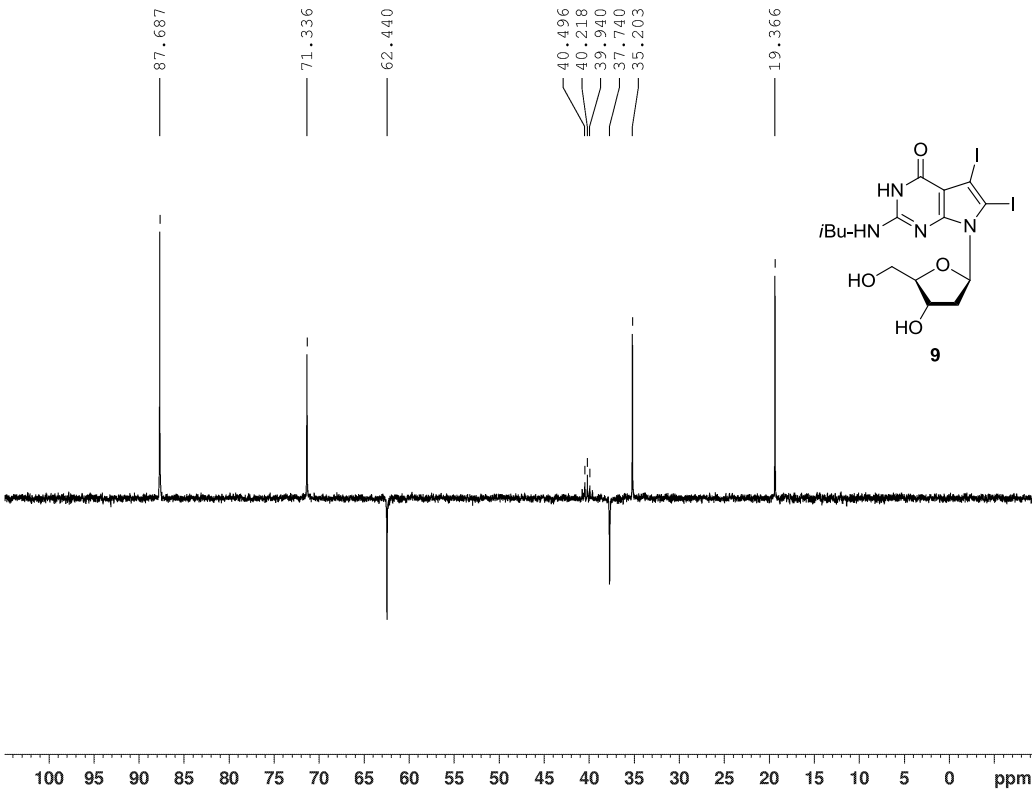

Figure 50. DEPT-135 NMR spectrum of compound **9**.

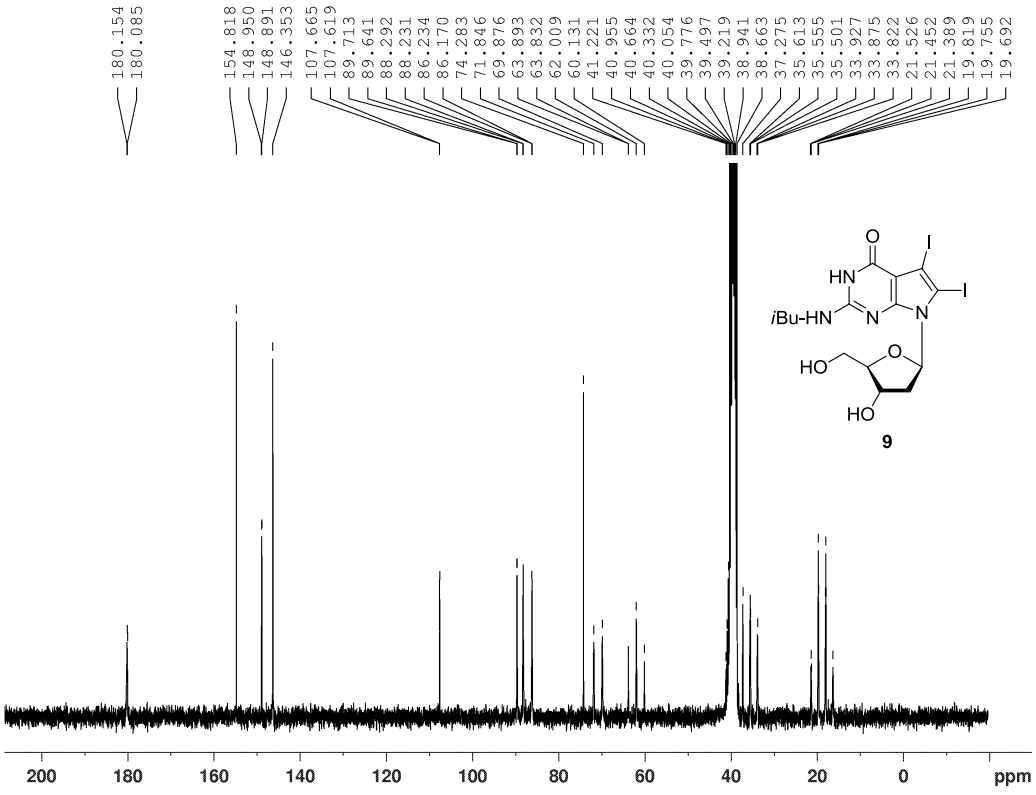

Figure 51. ^{1}H-^{13}C gated-decoupled NMR spectrum of compound **9**.

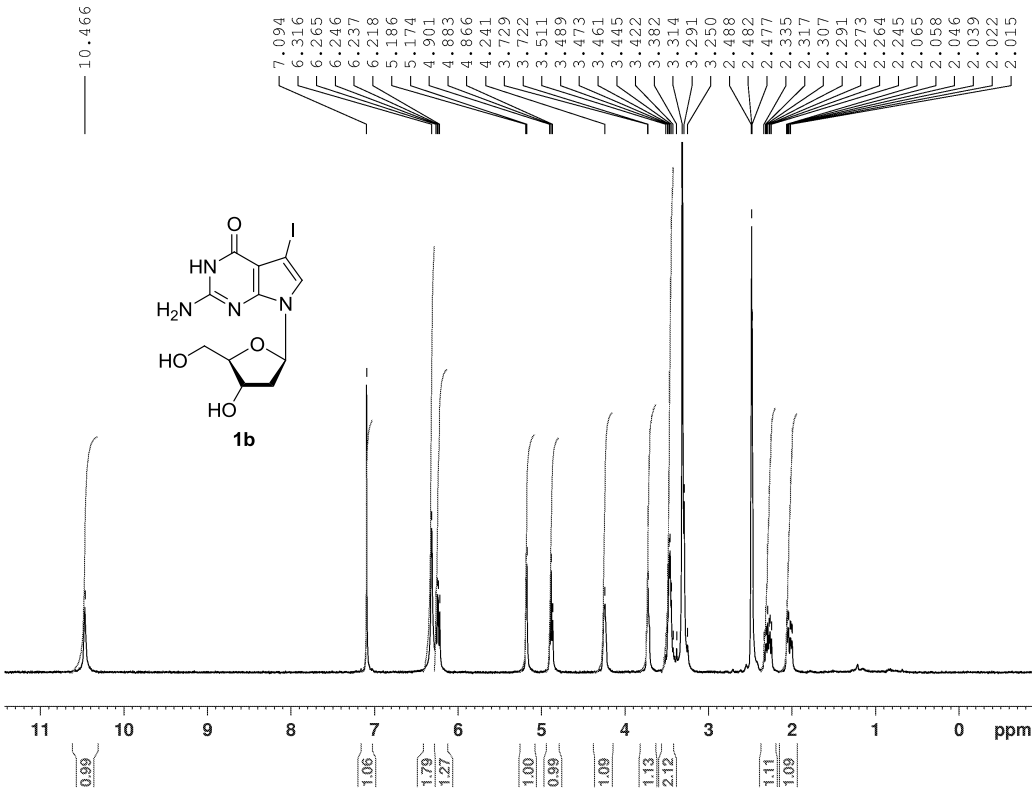

Figure 52. ^{1}H NMR spectrum of compound **1b**.

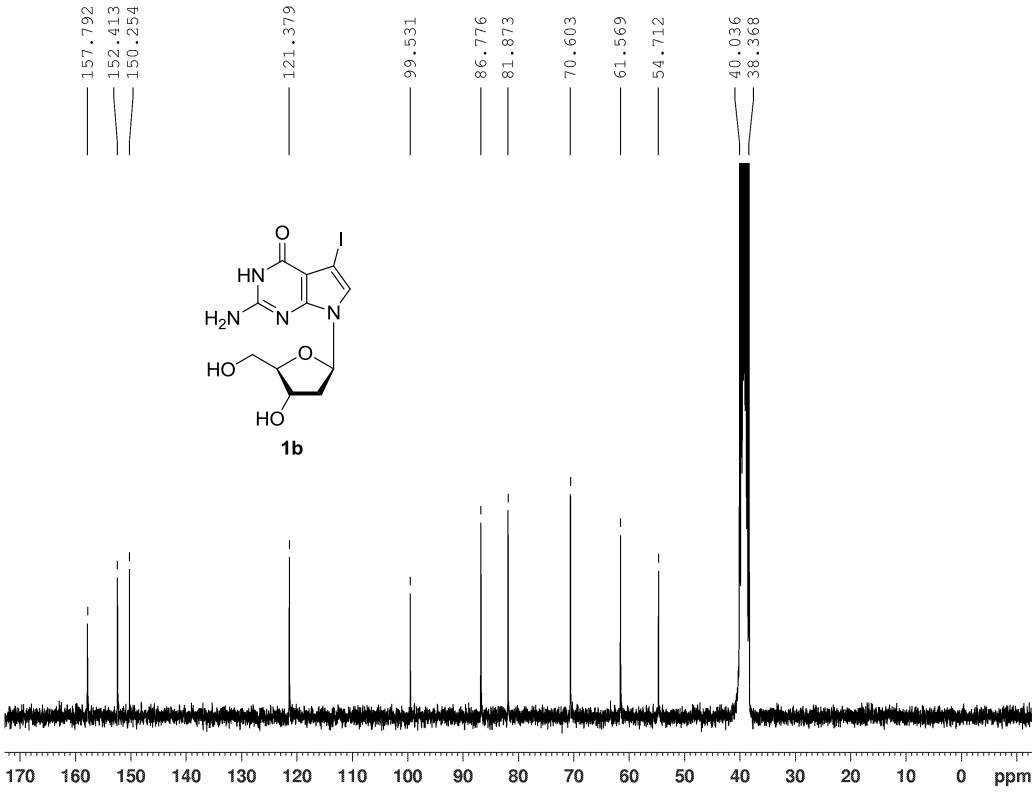

Figure 53. ^{13}C NMR spectrum of compound **1b**.

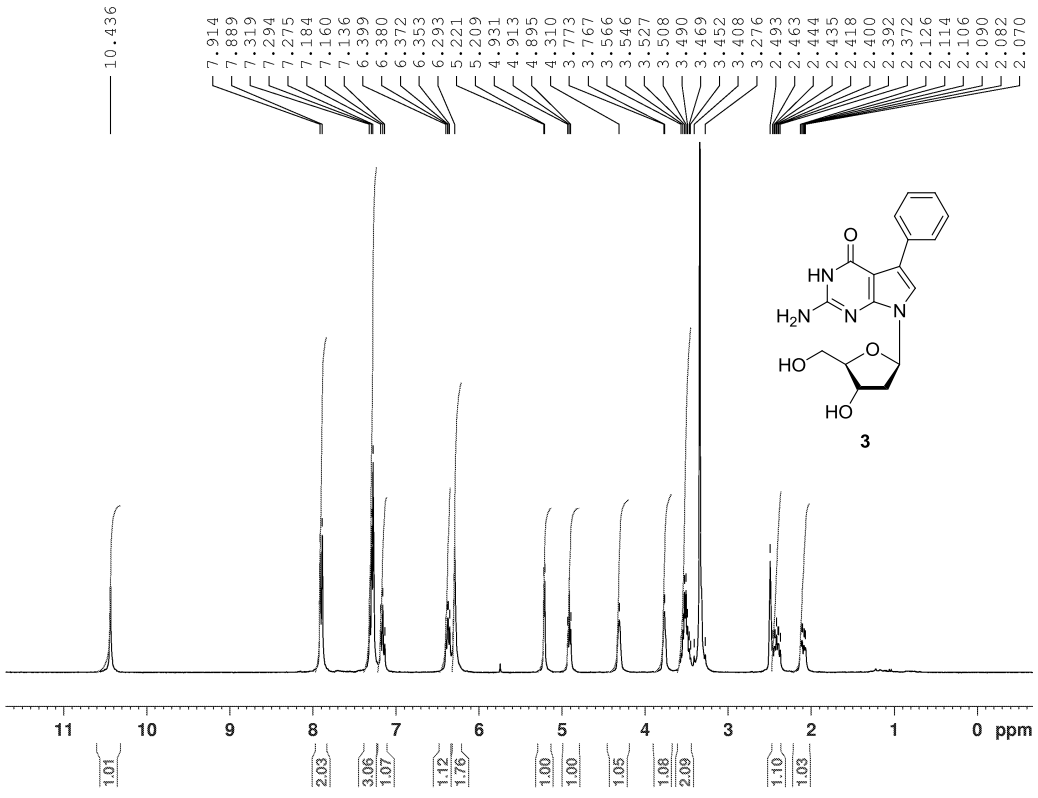

Figure 54. ^{1}H NMR spectrum of compound **3**.

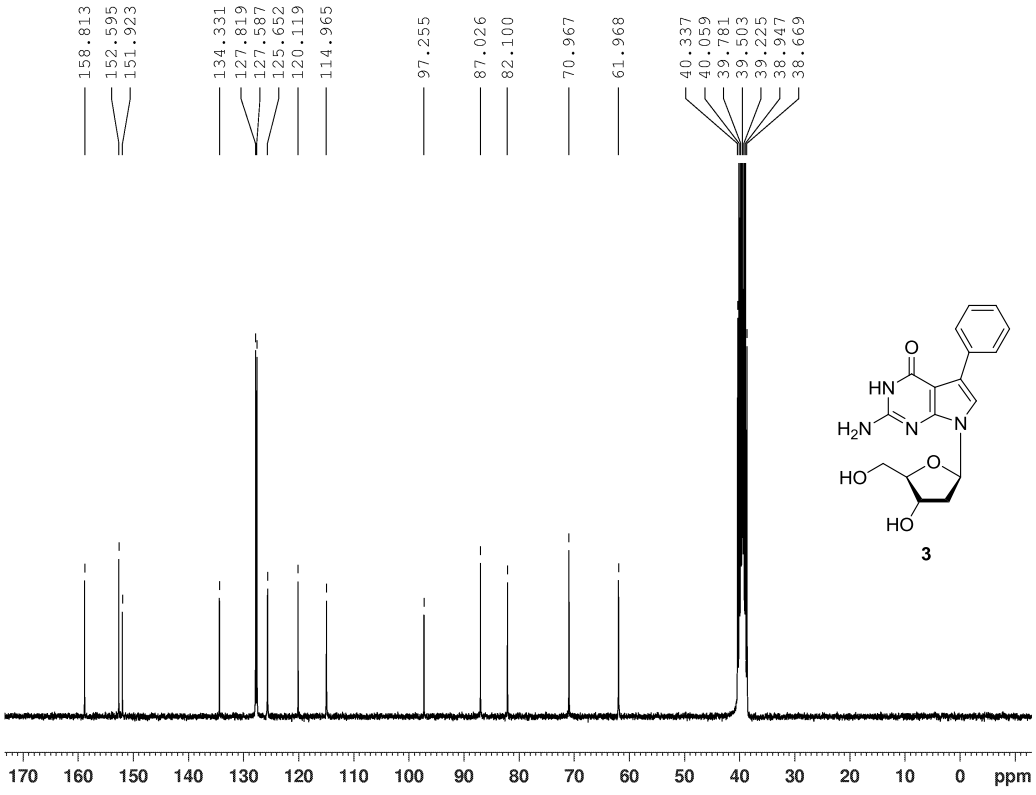

Figure 55. ^{13}C NMR spectrum of compound **3**.

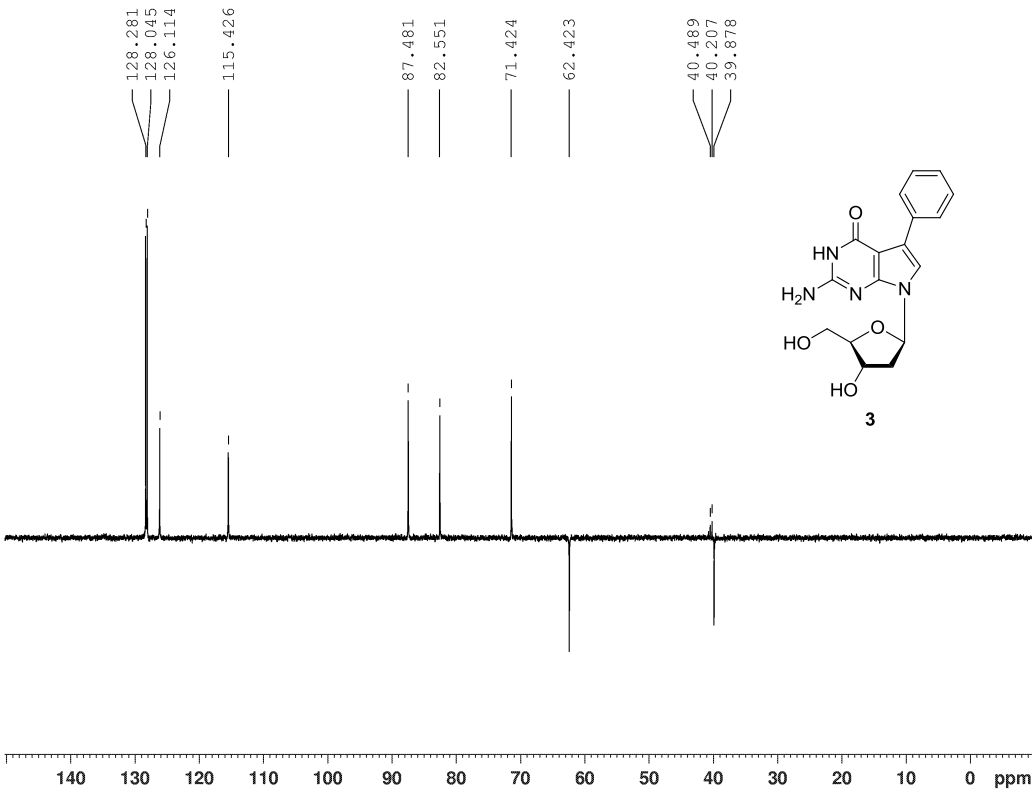

Figure 56. DEPT-135 NMR spectrum of compound **3**.

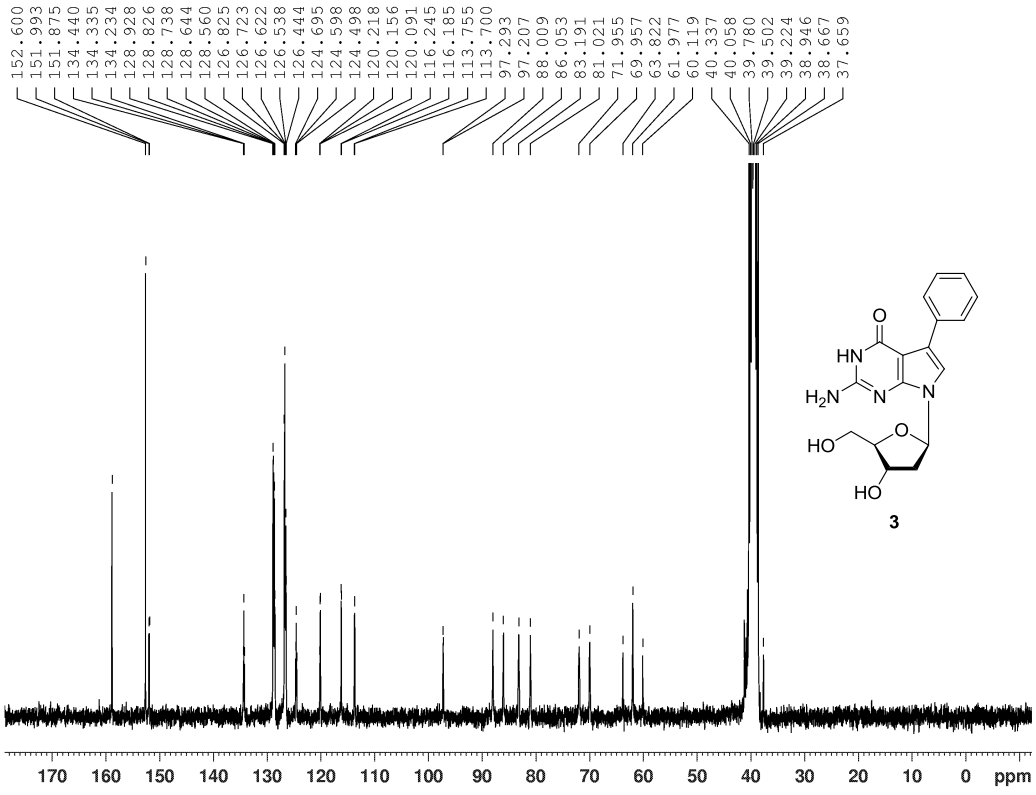

Figure 57. ^{1}H-^{13}C gated-decoupled NMR spectrum of compound **3**.

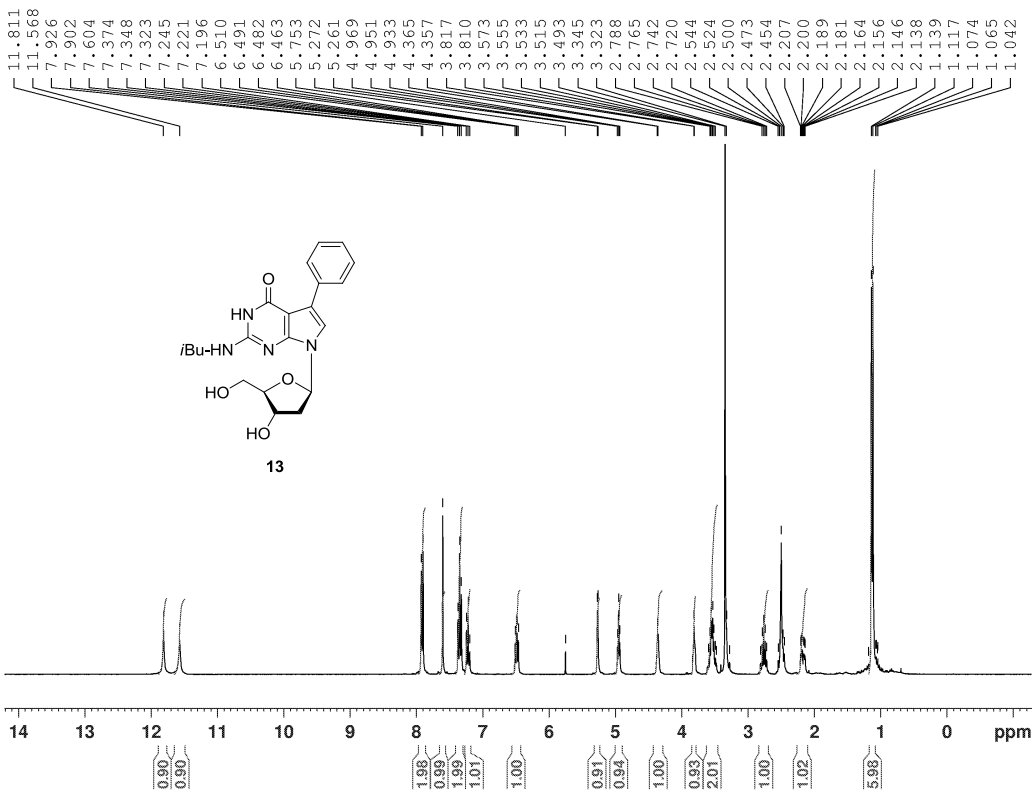

Figure 58. ^{1}H NMR spectrum of compound **13**.

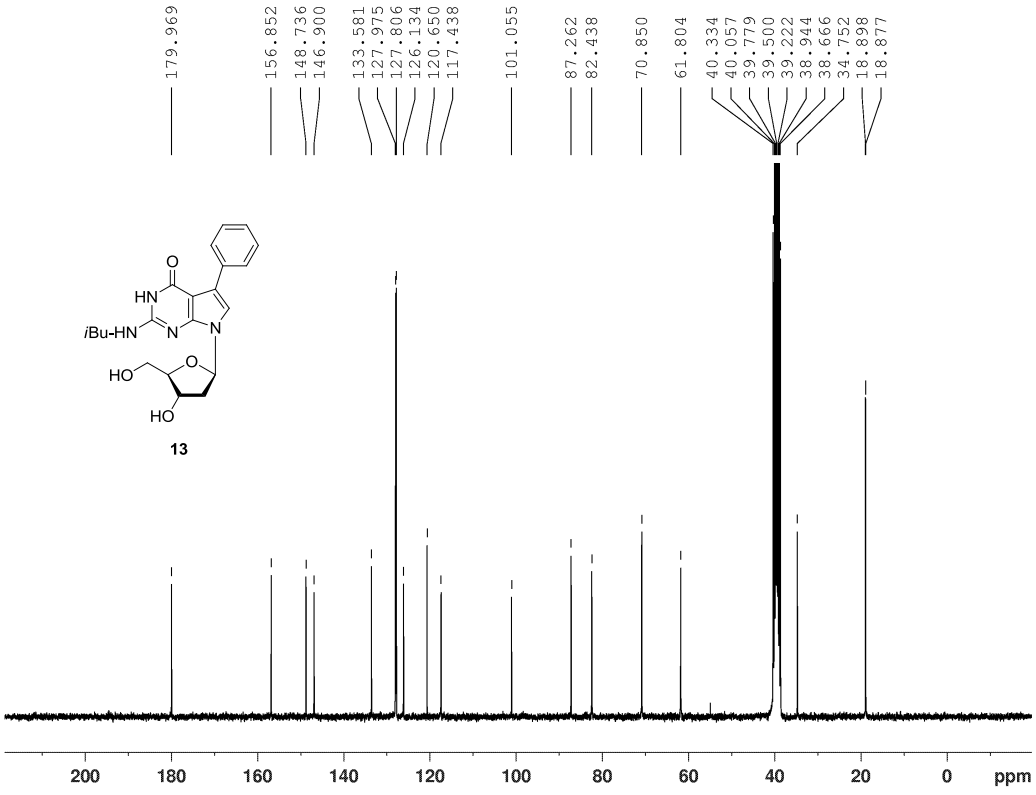

Figure 59. ^{13}C NMR spectrum of compound **13**.

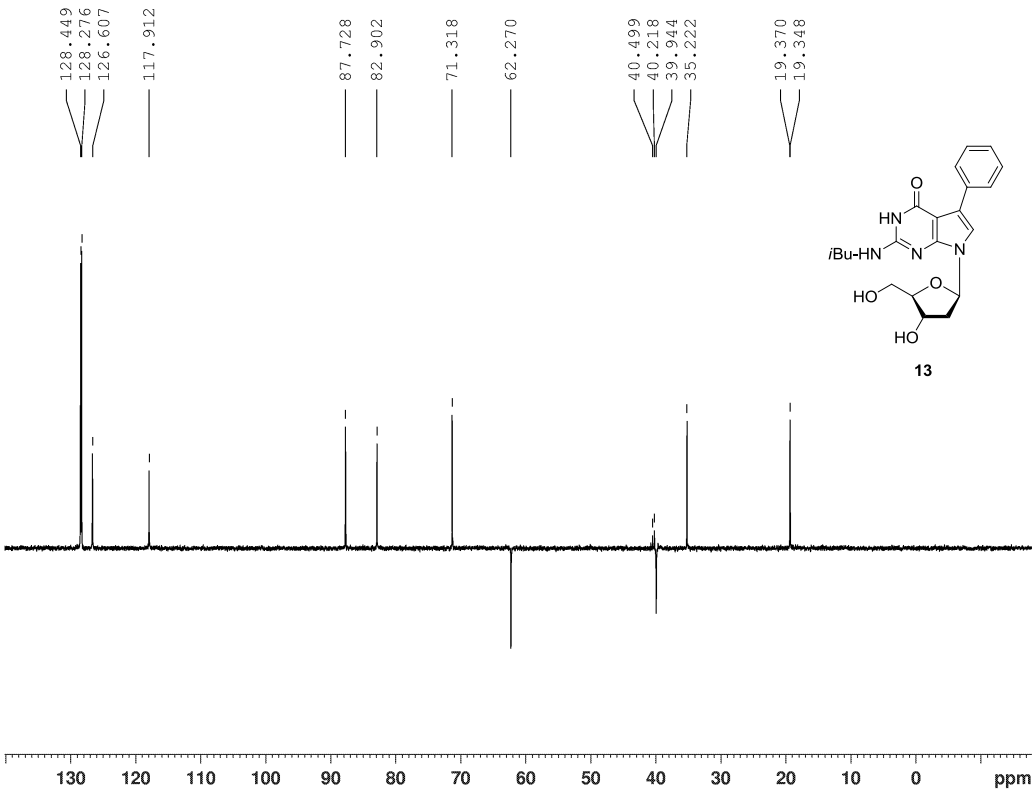

Figure 60. DEPT-135 NMR spectrum of compound **13**.

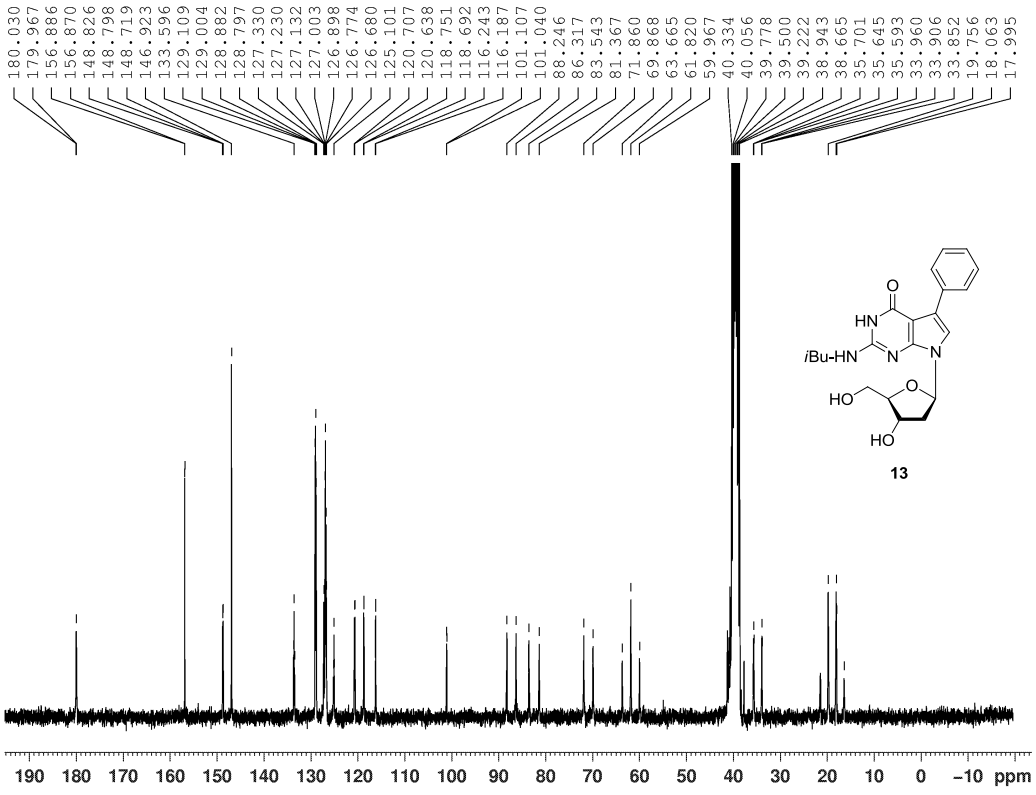

Figure 61. ^{1}H-^{13}C gated-decoupled NMR spectrum of compound **13**.

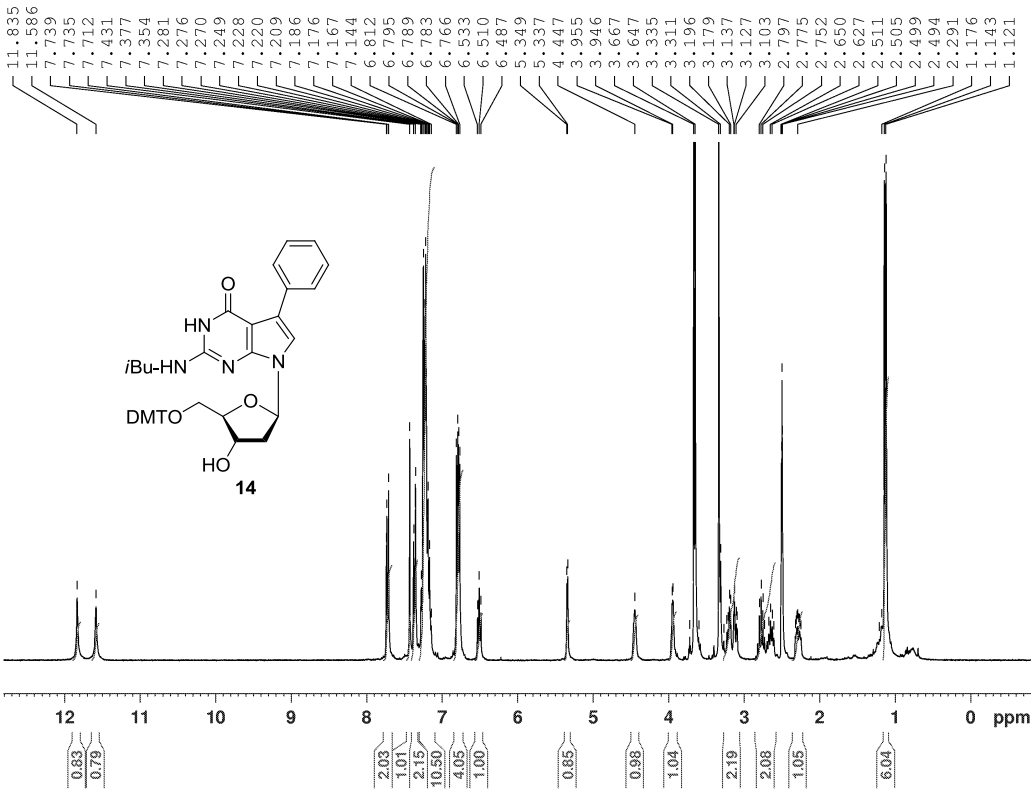

Figure 62. ^{1}H NMR spectrum of compound **14**.

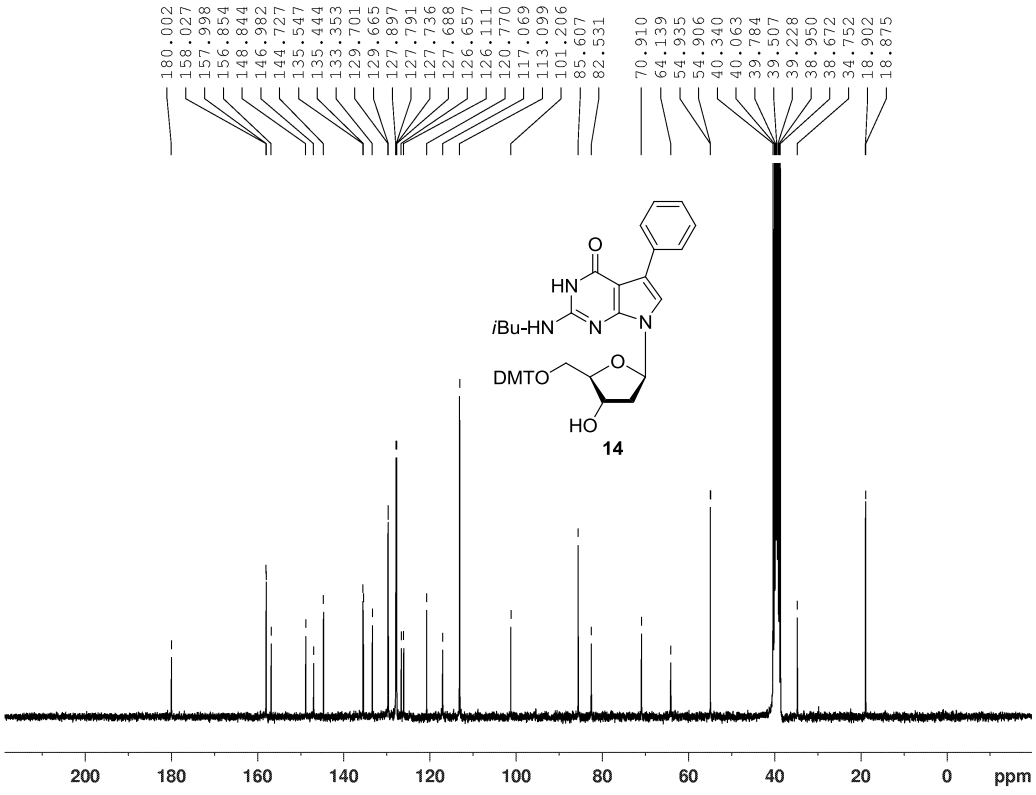

Figure 63. ^{13}C NMR spectrum of compound **14**.

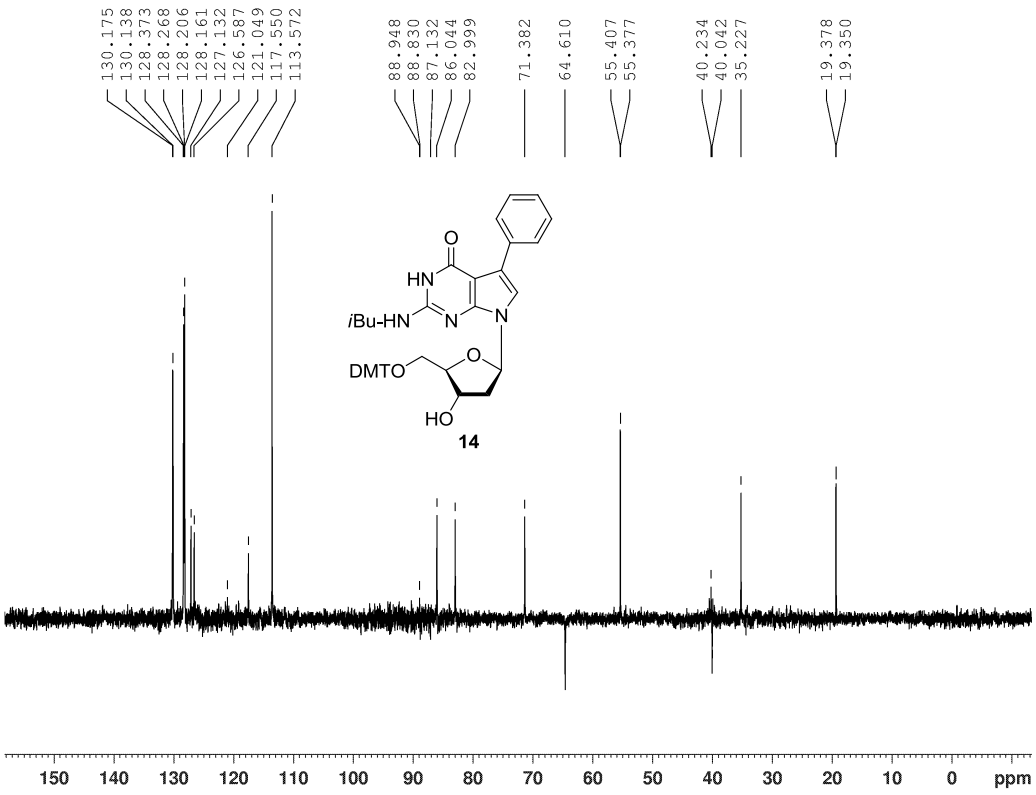

Figure 64. DEPT-135 NMR spectrum of compound **14**.

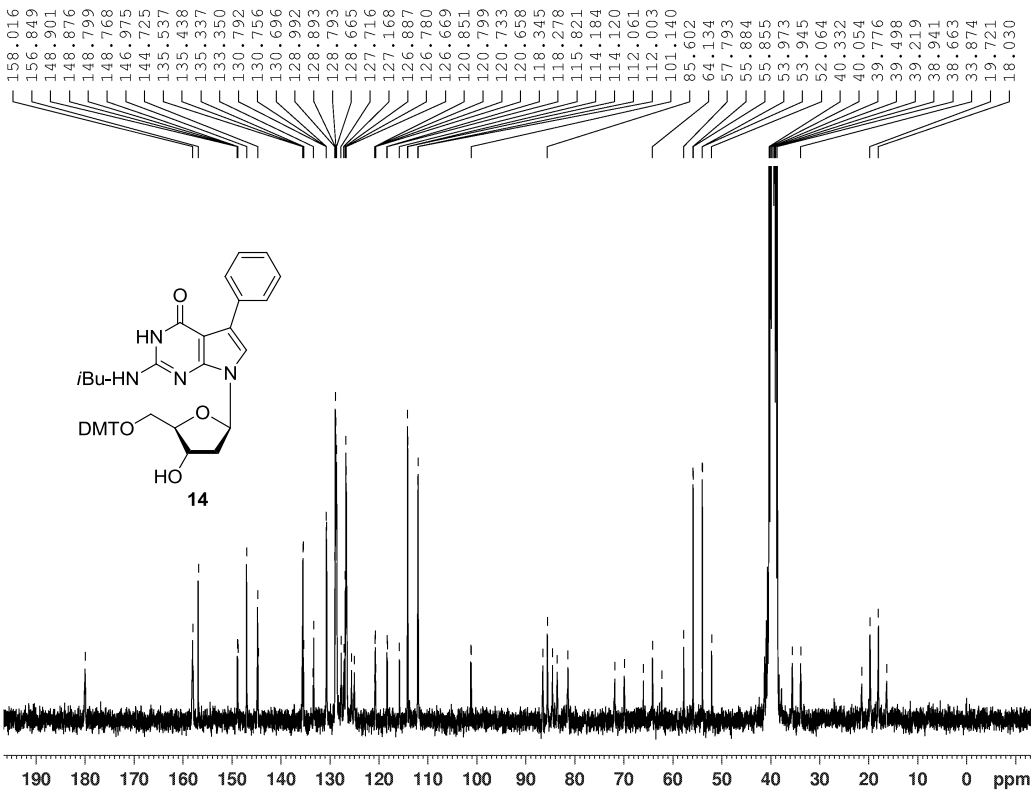

Figure 65. ^{1}H-^{13}C gated-decoupled NMR spectrum of compound **14**.

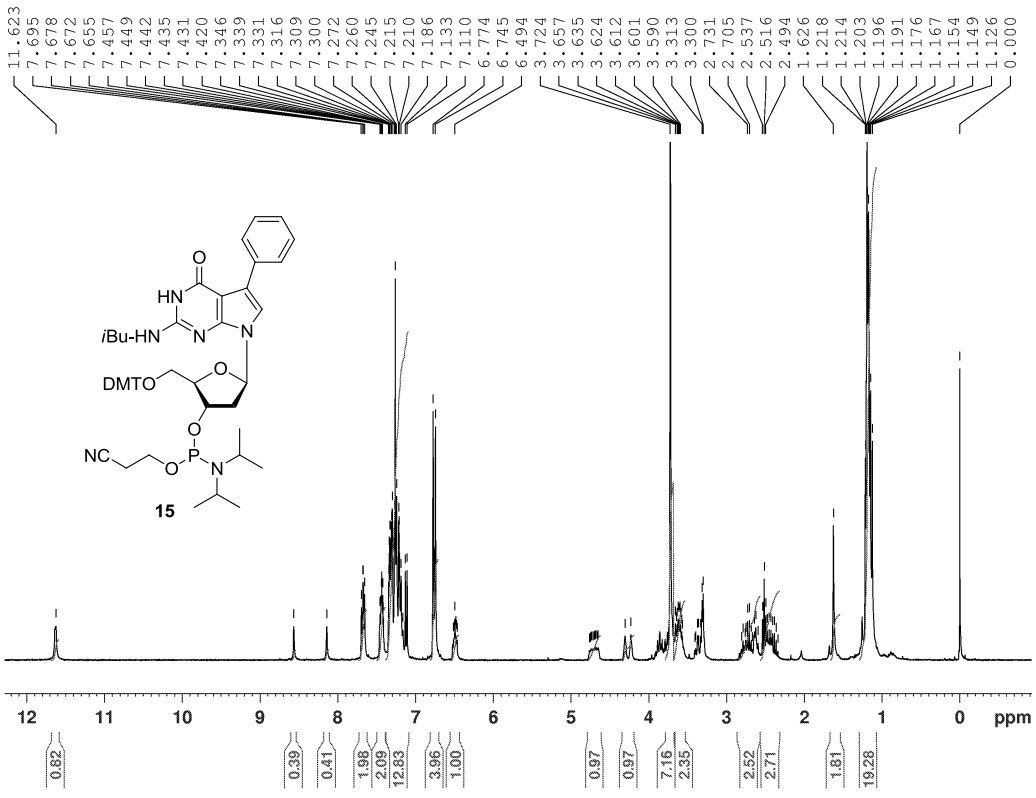

Figure 66. ^{1}H NMR spectrum of compound **15**.

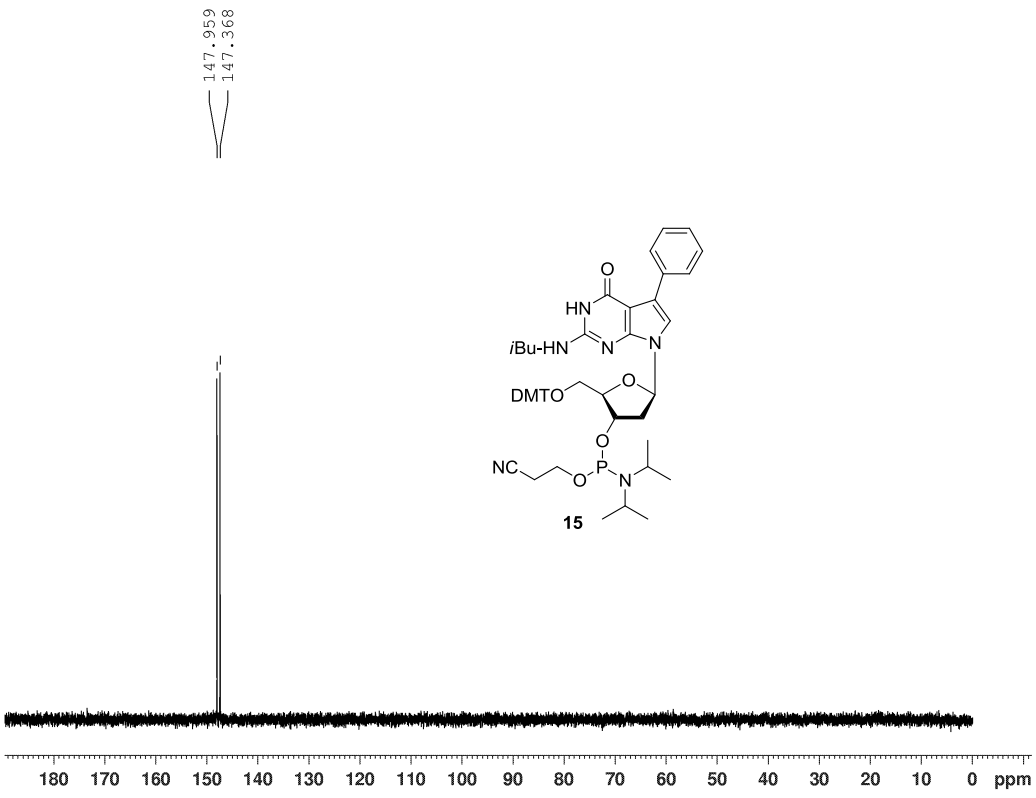

Figure 67. ^{31}P NMR spectrum of compound **15**.

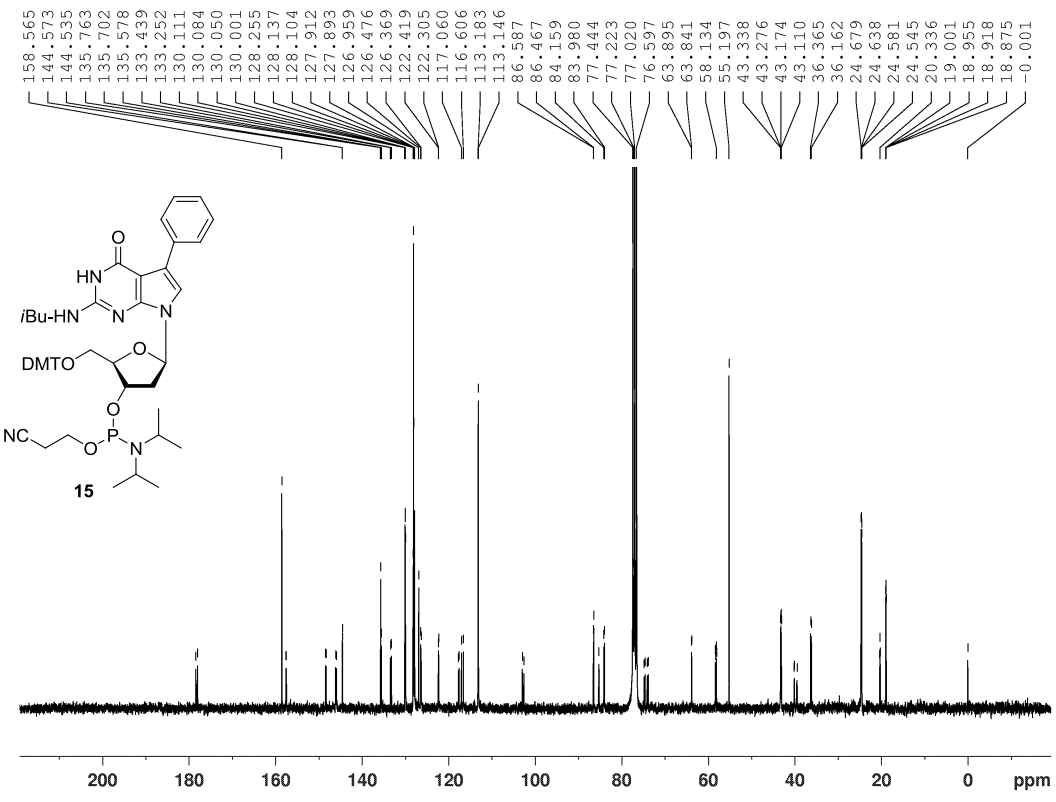

Figure 68. ^{13}C NMR spectrum of compound **15**.

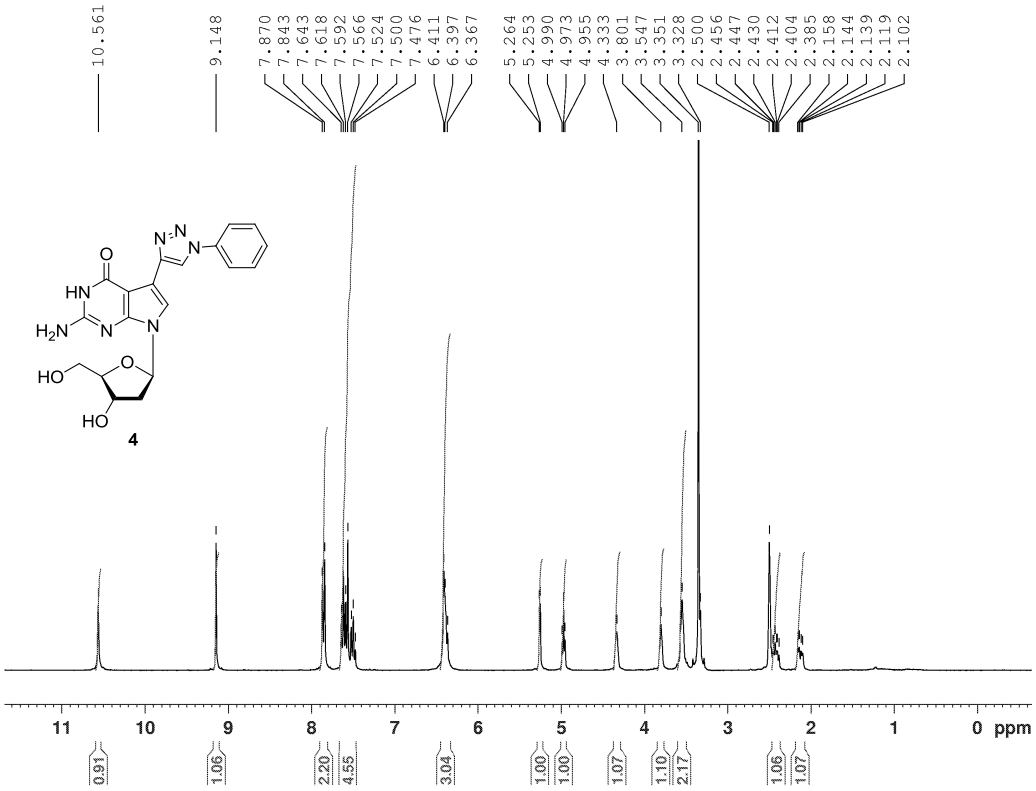

Figure 69. ^{1}H NMR spectrum of compound **4**.

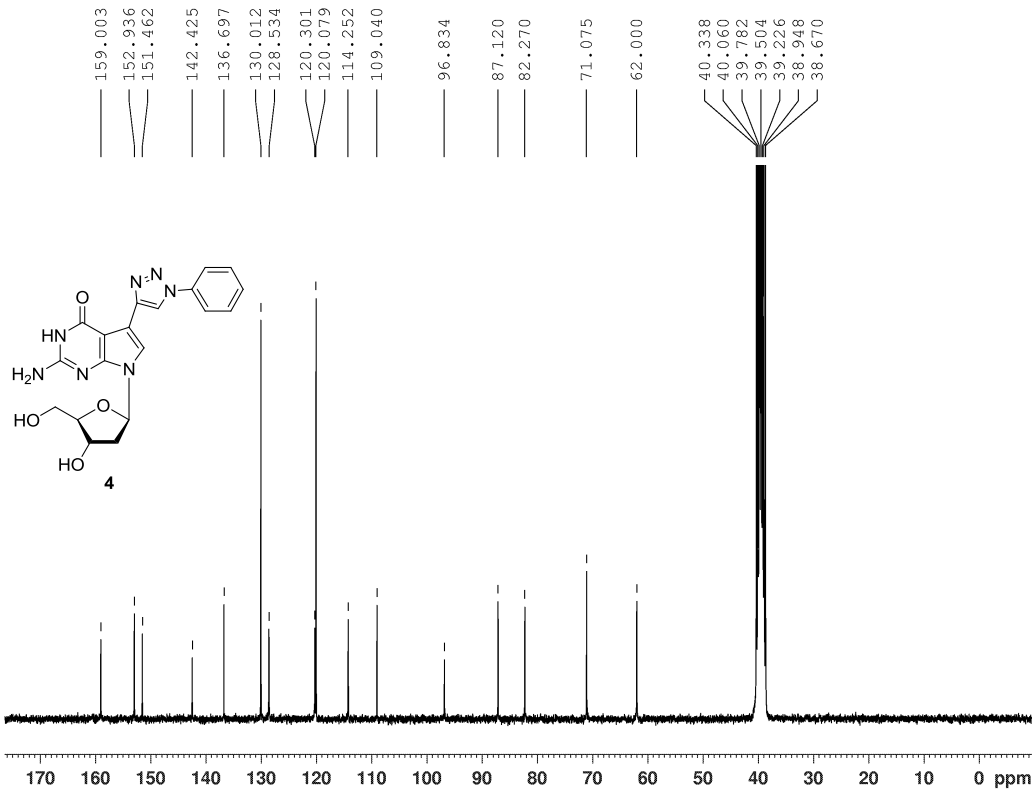

Figure 70. ^{13}C NMR spectrum of compound **4**.

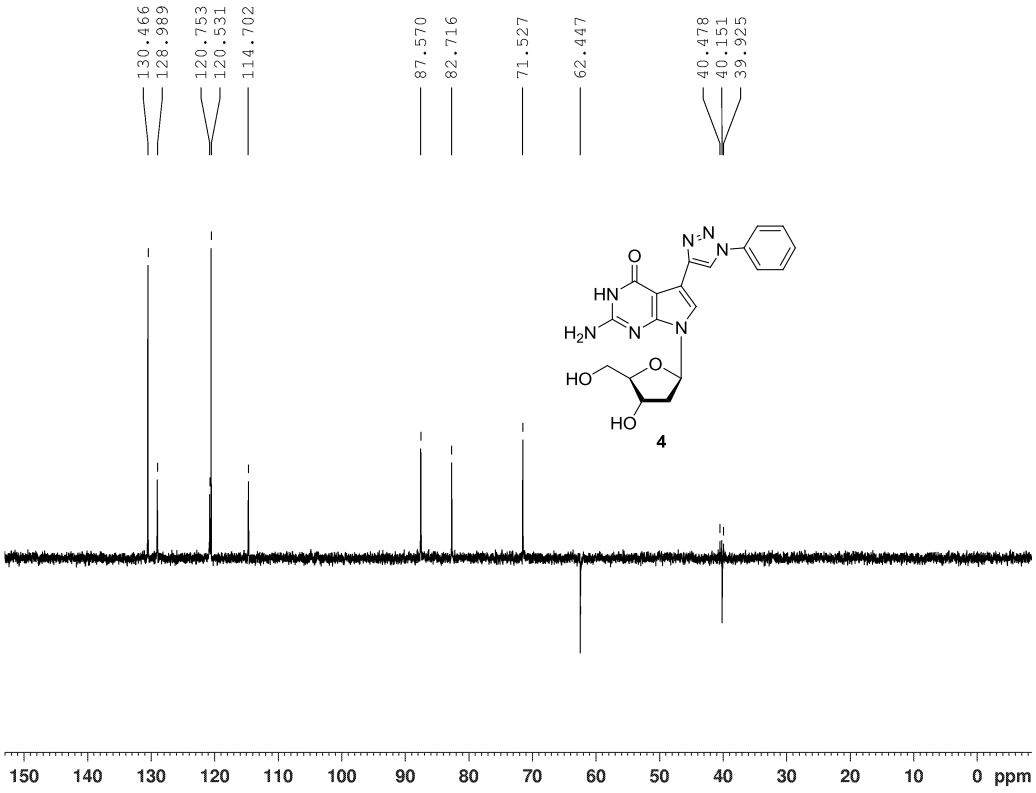

Figure 71. DEPT-135 NMR spectrum of compound **4.**

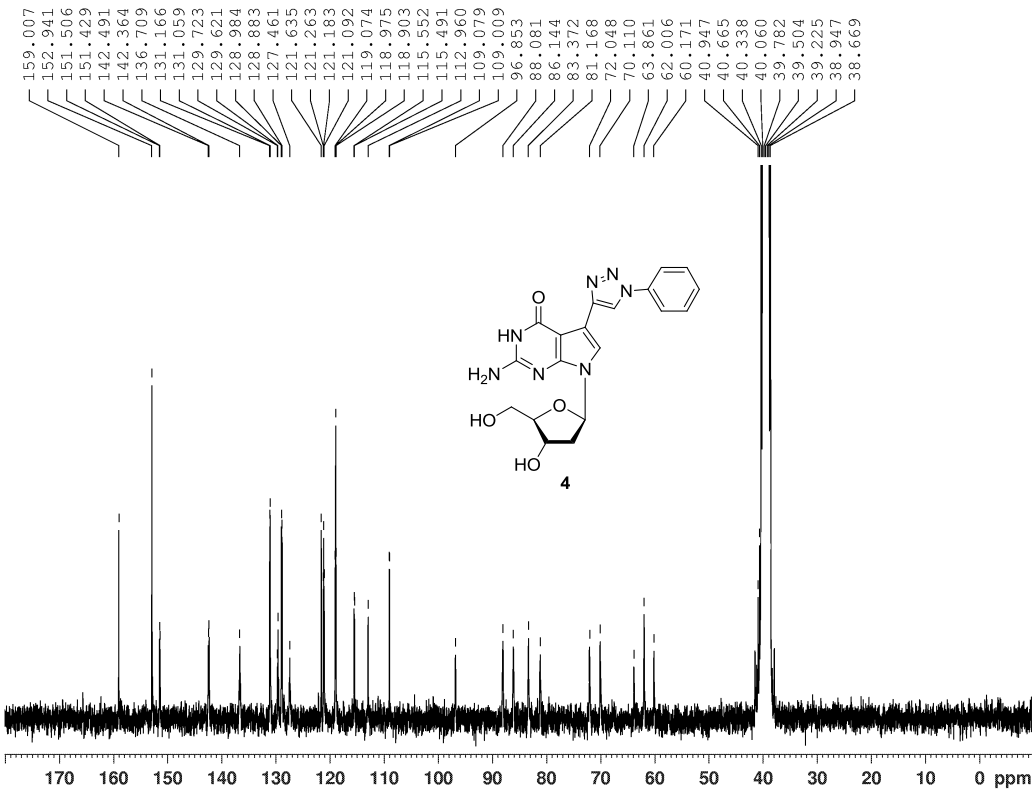

Figure 72. ^{1}H-^{13}C gated-decoupled NMR spectrum of compound **4.**

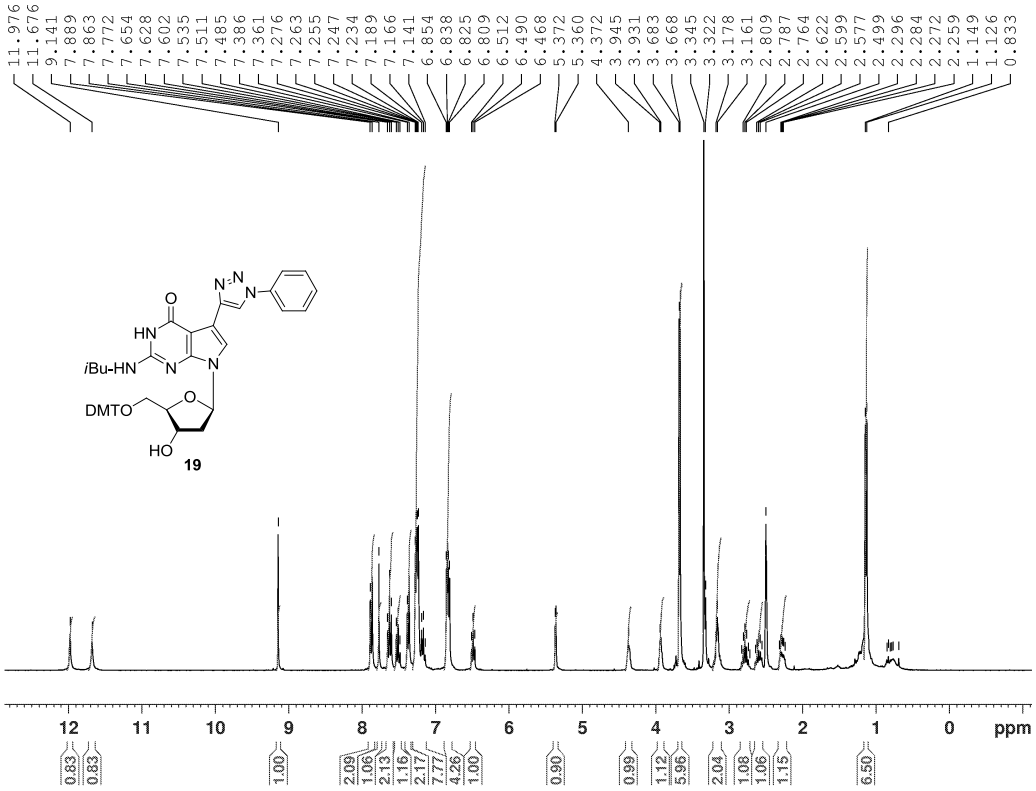

Figure 73. ^{1}H NMR spectrum of compound **19**.

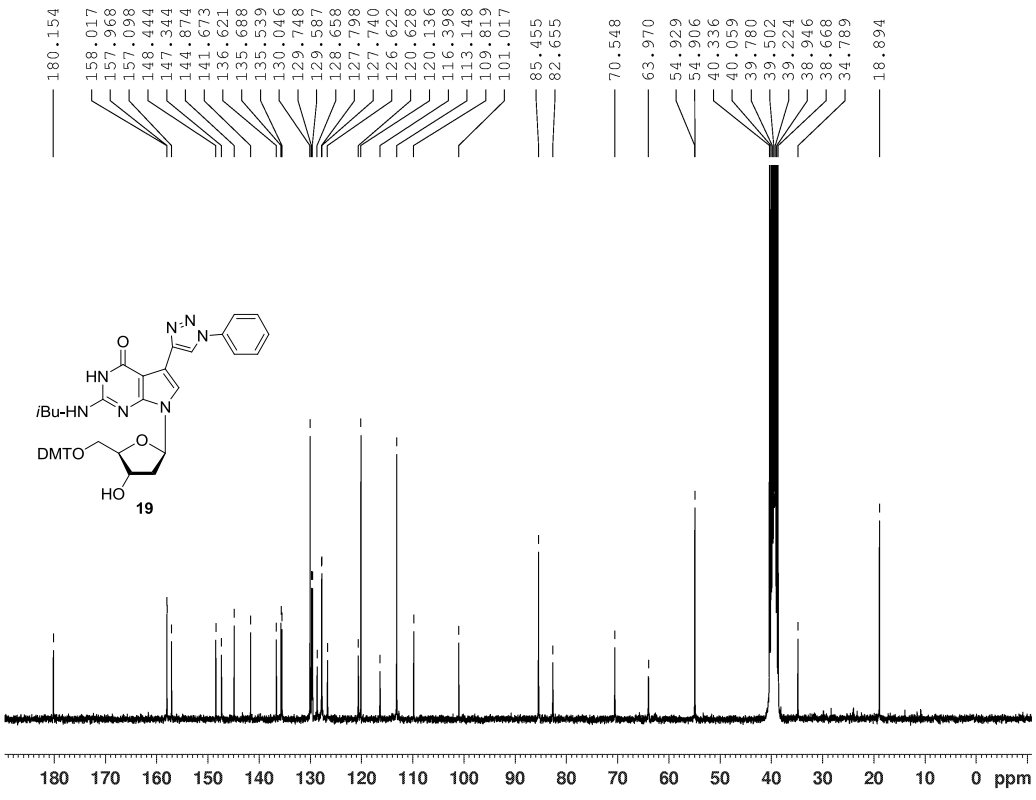

Figure 74. ^{13}C NMR spectrum of compound **19**.

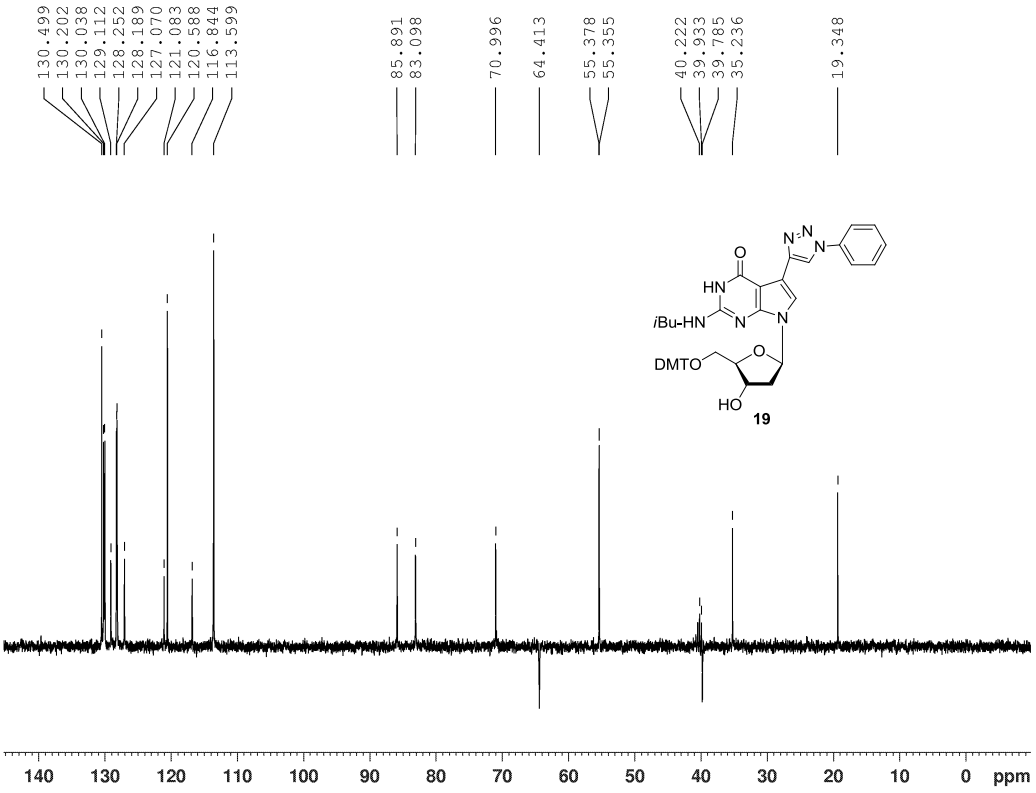

Figure 75. DEPT-135 NMR spectrum of compound **19**.

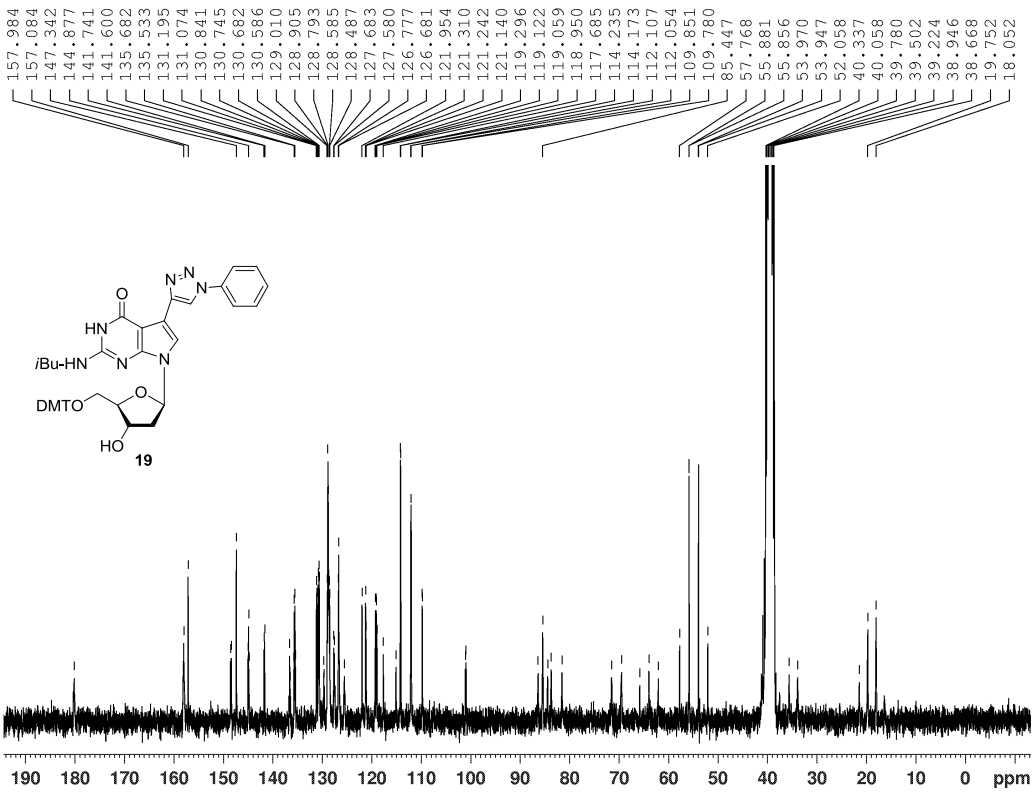

Figure 76. ^{1}H-^{13}C gated-decoupled NMR spectrum of compound **19**.

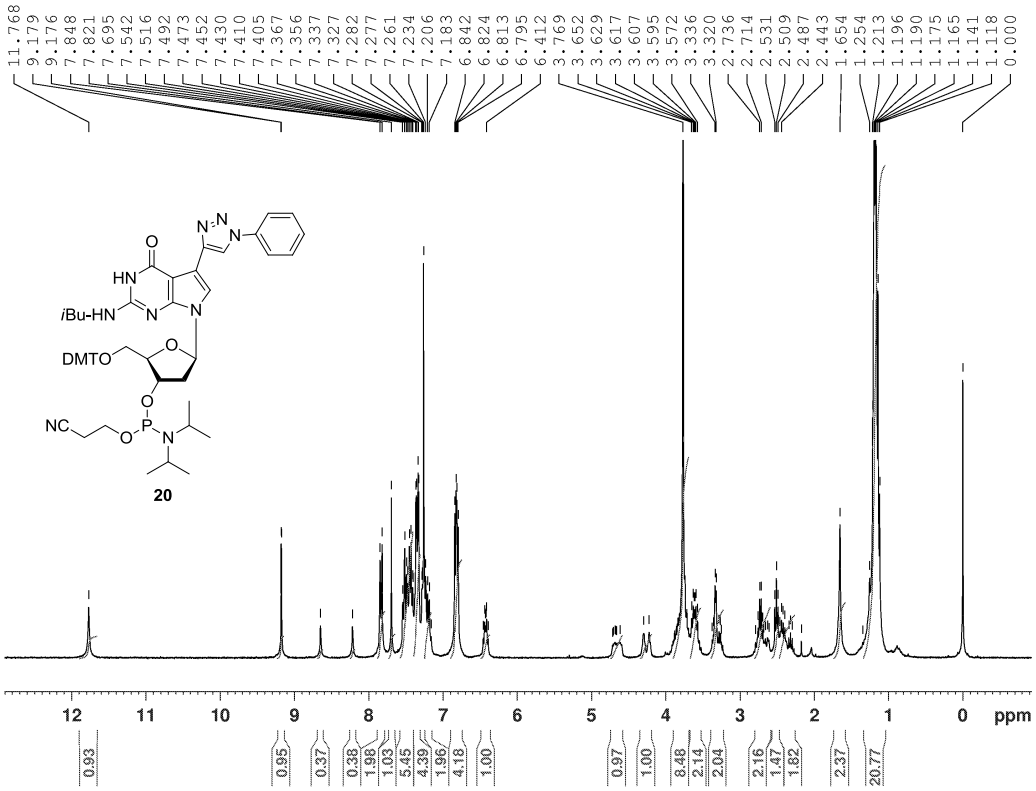

Figure 77. ^{1}H NMR spectrum of compound **20**.

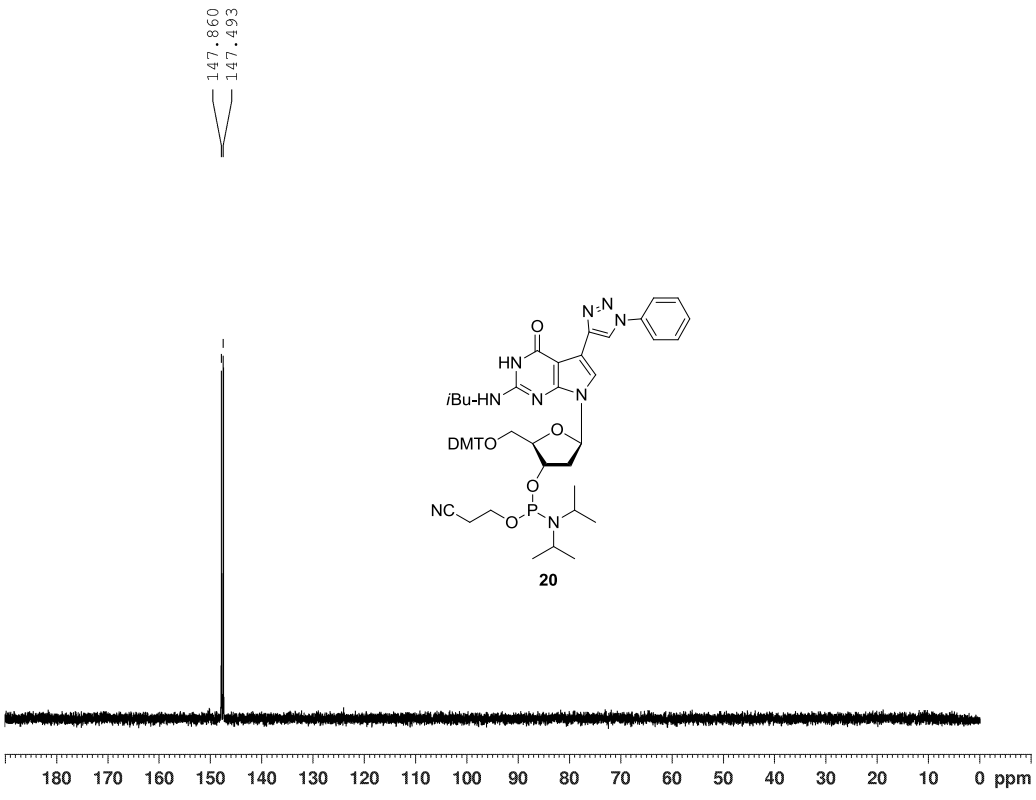

Figure 78. ^{31}P NMR spectrum of compound **20**.

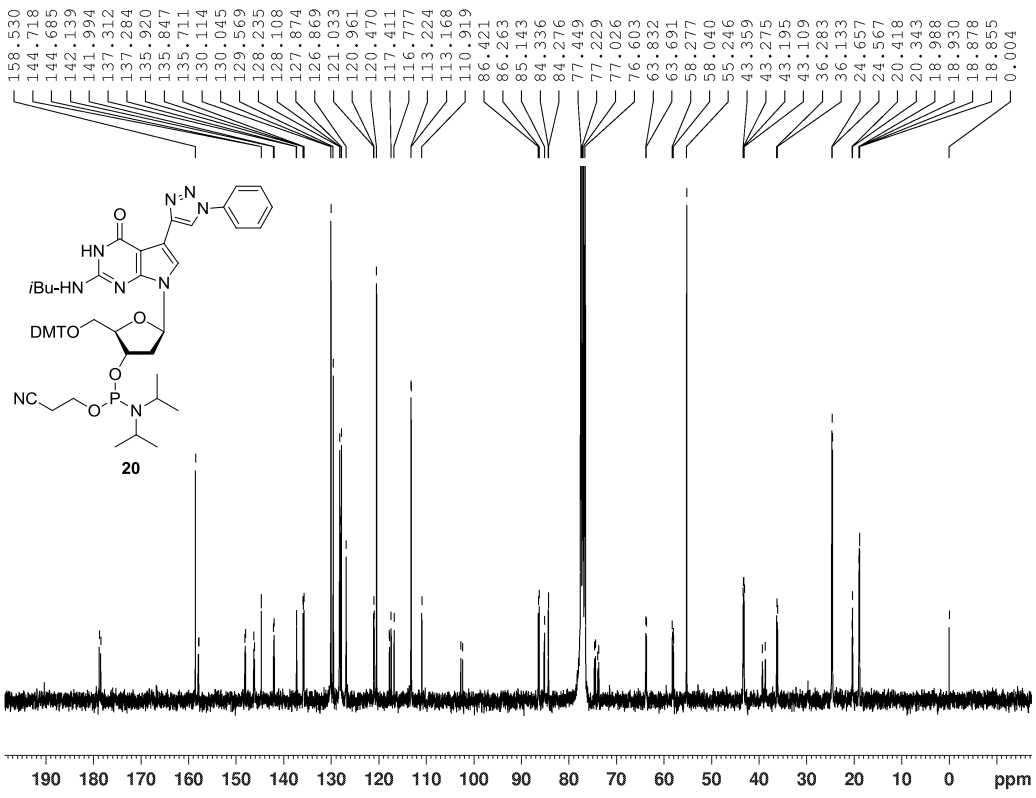

Figure 79. ^{13}C NMR spectrum of compound **20**.